Geological Society of America
Special Paper 409
2006

Geomorphological, depositional, and foraminiferal indicators of late Quaternary tectonic uplift in Iskenderun Bay, Turkey

Valentina Yanko-Hombach*
Avalon Institute of Applied Science, Charleswood Technology Center, 3227 Roblin Boulevard, Winnipeg MB R3R 0C2, Canada
Hayrettin Koral*
Department of Geology, Istanbul University, Avcilar 34850, Istanbul, Turkey
Niyazi Avşar*
Department of Geological Engineering, Çukurova University, Balcali 01330, Adana, Turkey
Irena Motnenko*
Avalon Institute of Applied Science, Charleswood Technology Center, 3227 Roblin Boulevard, Winnipeg MB R3R 0C2, Canada
Mary McGann*
U.S. Geological Survey, Menlo Park, California 94025, USA

ABSTRACT

Iskenderun Bay is a major shallow embayment in the eastern part of the Mediterranean Sea, where the African and Anatolian Plates converge. This tectonically active basin was investigated for oceanographic, sedimentological, geochemical, and foraminiferal parameters. On the basis of the data acquired, the distribution of living and fossil foraminifera in 284 grab and 54 gravity core samples was determined, the basin floor bathymetry of the bay constructed, radiocarbon ages of sediments and fossils ascertained, and depositional environments reconstructed. It has been discovered that for the last 13.5 k.y., water masses were stratified and sedimentation was discontinuous within the basin, which is characterized by irregular sea bottom morphology. The sedimentation rate was very slow, varying in time and space from 0 to 0.012 cm yr^{-1}. The foraminiferal distributions were spatially varied and discontinuous and indicate a reversal from deep to shallow marine conditions in the cores. These irregularities were attributed to active tectonics in the bay and a major tectonic uplift of the bay since the late Pleistocene.

Keywords: Iskenderun Bay, late Quaternary foraminifera, lithotypes, tectonics, sedimentation rate

*E-mails: Yanko-Hombach (corresponding author)—valyan@avalon-institute.org; Koral—hkoral@istanbul.edu.tr; Avşar—avsarn@mail.cu.edu.tr; Motnenko—irmot@avalon-institute.org; McGann—mmcgann@usgs.gov.

Yanko-Hombach, V., Koral, H., Avşar, N., Motnenko, I., and McGann, M., 2006, Geomorphological, depositional, and foraminiferal indicators of late Quaternary tectonic uplift in Iskenderun Bay, Turkey, *in* Dilek, Y., and Pavlides, S., eds., Postcollisional tectonics and magmatism in the Mediterranean region and Asia: Geological Society of America Special Paper 409, p. 591–614, doi: 10.1130/2006.2409(27). For permission to copy, contact editing@geosociety.org. ©2006 Geological Society of America. All rights reserved.

INTRODUCTION

In 1991, a multidisciplinary field and experimental research program was set up to use benthic foraminifera as environmental tracers of heavy metal pollution in the eastern Mediterranean. The international project AVICENNE (1993–1996) that constituted a part of this program aimed to investigate the pollution along the Turkish and northern Israeli coasts by using benthic foraminifera (AVICENNE Annual Report, 1993, 1995, 1996; Basso et al., 1994; Yanko et al., 1998; Basso and Spezzaferri, 2000). As a part of the campaign along the Turkish coast, short gravity cores were collected in various parts of Iskenderun Bay to supplement a wider environmental investigation of the effects of heavy metal pollution on benthic foraminiferal populations in the surface sediments. It was principally hoped that these cores would show how the foraminiferal populations responded to increasing anthropogenic pollution over historical time, because it had been assumed that there should be only small differences in the foraminiferal assemblages of these short cores taken from comparable depths in the subsiding (Aksu et al., 1992) shallow bay. However, this turned out not to be the case at all. The Iskenderun Bay data presented a greater complexity in unraveling foraminiferal, depositional, and geomorphological data than would be initially expected in an ordinary sedimentary basin, implying that parameters related to the active tectonic setting of the basin are influential (Kronfeld et al., 1996).

There are two contradictory views of the late Quaternary evolution of Iskenderun Bay. Subsidence is suggested on the basis of seismic profiling and aerial photographs showing that since ca. 0.62 Ma, the continental shelf of the northern Mediterranean Sea, Iskenderun Bay in particular, was formed by superimposed deltaic successions (depositional sequences) separated by major erosional unconformities. This has been interpreted as the formation and modification of the deltas in response to glacioeustatic sea level fluctuations during the Pleistocene, superimposed upon a continuous basin subsidence at a rate of 0.33×10^{-3} m yr^{-1} (Aksu et al., 1992). Neither sampling nor direct chronological control for the depositional sequence has been performed.

Alternatively, uplift argues that delta progradation and architecture are not restricted to a downward-sinking basin (Kronfeld et al., 1996; Koral et al., 1999, 2001). Such features require a difference in absolute levels of relative changes between sea and land surfaces, and they can be formed where the sea level rise or fall is greater than the movement of the land. During late Glacial to post-Glacial time, when cycles of relatively large and rapid glacioeustatic sea level oscillations were especially pronounced (Fairbanks, 1989), such features could have been formed as well by continuous uplift of the Iskenderun Bay floor.

The main goal of this article is to present geomorphological, depositional, microfaunal (foraminifera), geochemical, and ^{14}C records as evidence of late Quaternary paleoceanographic and tectonic reconstructions in support of the "uplift hypothesis" in Iskenderun Bay.

PHYSIOGRAPHIC, GEOLOGICAL, AND TECTONIC SETTINGS

Iskenderun Bay is a large, though shallow, embayment of the southeastern coastline of Turkey (Fig. 1A) that lies in the easternmost part of the Mediterranean Sea at the edge of the Turkish-Anatolian Plate, immediately southwest of the Africa-Arabia-Anatolia triple junction (Dewey et al., 1986). It is located between the southeastern coast of Asia Minor and the Arabian Peninsula and forms the intermountain depression between the Missis-Andirin and the Amanos massifs (Hall et al., 1994). The bay is a rectangular (60 km long and 35 km wide; Yılmaz et al., 1992; Yılmaz and Gürer, 1996), shallow (maximum water depth 87 m), bath-shaped asymmetric depression tilted toward the Dead Sea fault zone (DSFZ, Fig. 1A).

The Ceyhan River, originating in the Taurus Mountains at 2200 m height to the north, flows southwest into Iskenderun Bay. Excluding ephemeral streams located in the eastern and southern hinterland (Ergin et al., 1996), it is the principal supplier of freshwater (14×10^9 m^3 yr^{-1}; Cullen et al., 2002) and silisiclastic sediments (5462×10^3 t yr^{-1}; Aksu et al., 1992) to the bay. The river has built a prominent delta complex off the northwest coast of the bay, with a large fluvial coastal plain characterized by a delta mouth, lagoons, marshes, and abandoned channels (Bal and Demirkol, 1987). In the mid-Holocene, the delta was abandoned and replaced to the south (Spezzaferri et al., 2000).

Water circulation in the bay is highly dynamic and seasonally dependent (Ergin et al., 1996). In the summer, currents of open-sea waters enter the bay from the northwest and form clockwise and counterclockwise gyres (Iyiduvar, 1986; Ergin et al., 1996). During the winter, open-sea waters enter the bay from the south-southwest and move toward the inner bay along the coast.

The geology of Iskenderun Bay and its coast is formed by Quaternary-age alluviums in the north and the northwest, by Miocene-age sedimentary rocks in the east and the west, and by ophiolitic, basic, and ultra-basic rock units in the east (Tolun and Pamir, 1975).

The bay is situated along the Eastern Anatolian fault (EAF) to the west of the Bitlis-Zagros suture (BZS) and to the east of the Cyprus arc (Fig. 1A; McKenzie, 1972; Nur and Ben-Avraham, 1978; Şengör et al., 1985; Bozkurt, 2001). The Bitlis-Zagros suture is a collision zone between the Arabia and Anatolia plates that arose from the terminal closure of the Bitlis Ocean nearby in the Late Pliocene–Quaternary (Şengör and Yılmaz, 1981; Robertson, 1998). The Cyprus arc is likewise a convergent plate boundary. Thus, Iskenderun Bay lies in an active convergent tectonic setting between the Anatolian and African plates (Şengör and Yılmaz, 1981; Şengör et al., 1985; Robertson, 1998). The left lateral strike-slip Eastern Anatolian fault that accommodates a part of the convergence comprises many faults of listric geometry in Iskenderun Bay (Aksu et al., 1992) and causes the deformation of the Quaternary succession

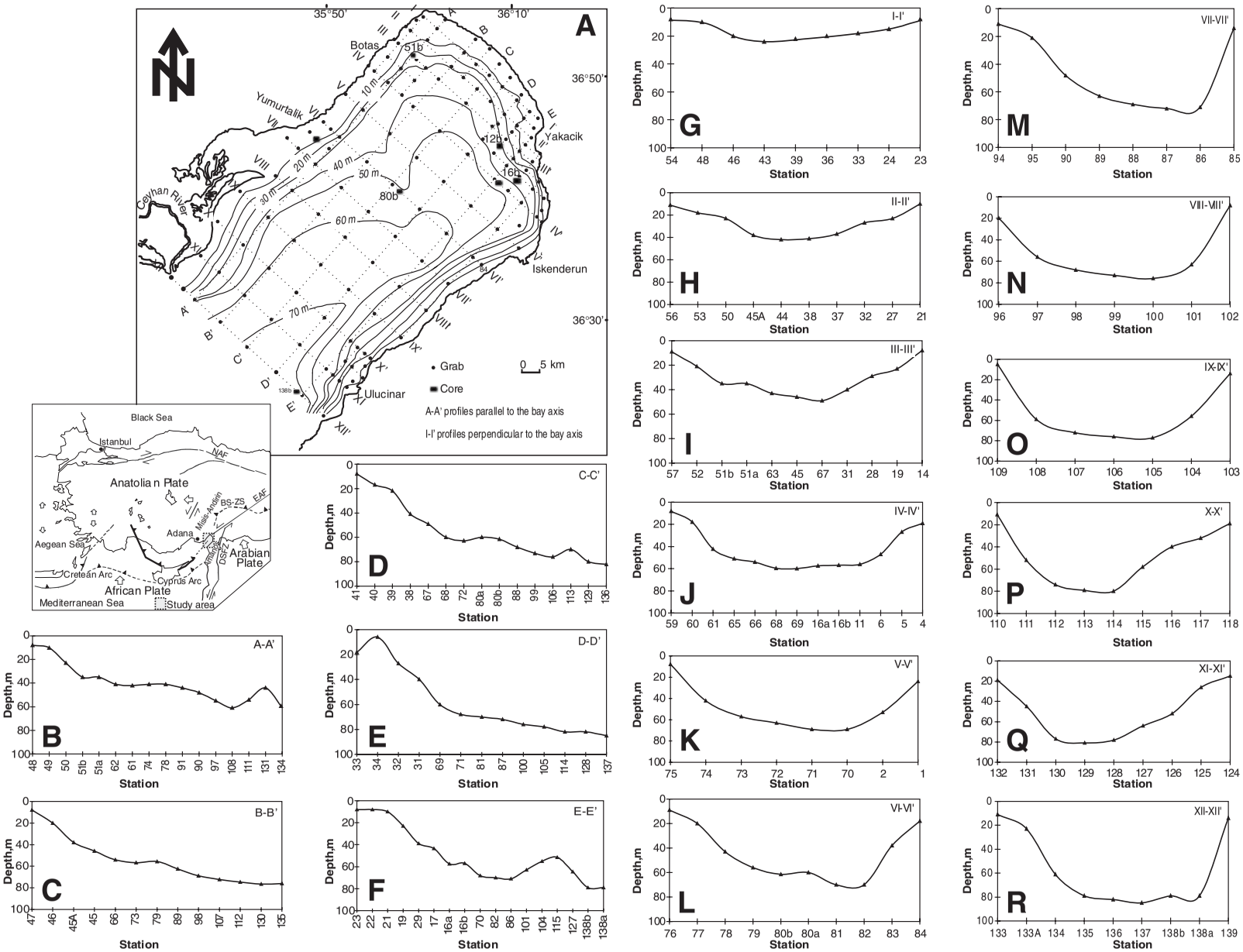

Figure 1. (A) Map of Iskenderun Bay showing the location of the study area, the bathymetry in meters, sampling profiles, and the grab (labeled black dots) and core (labeled black squares) locations. BZS—Bitlis-Zagros suture; DSFZ—Dead Sea fault zone; EAF—Eastern Anatolian fault; NAF—North Anatolian fault. (B–F) Cross-sections of the bottom obtained parallel to the shore showing the bottom morphology. Figure (G–R) Cross-sections of the bottom obtained perpendicular to the shore.

TABLE 1. FORAMINIFERAL PARAMETERS, ^{14}C, SEDIMENTATION RATE, $CaCO_3$ AND C_{ORG} CONTENTS IN CORE SEDIMENTS OF ISKENDERUN BAY

Core*	Water depth (m)	Sediment depth (cm)	Number of species	^{14}C age yr BP (uncorrected)	^{14}C age yr BP (calibrated)	Analysis no.	Sedimentation rate (cm/1000 yr)	$CaCO_3$ (%)	C_{org},%	$\delta^{13}C$ (‰) planktonic	$\delta^{13}C$ (‰) benthic	$\delta^{18}O$ (‰) planktonic	$\delta^{18}O$ (‰) benthic
12b	41.5	0–2	36	6620 ± 90	5512 ± 62	Ki-10405	0	21	0.9				
		10–12	24					24	1.1				
		20–22	25					27	0.8				
		30–32	31	12 390 ± 90	12 536 ± 124	Ki-10406	0	23	2.1				
		40–42	28					19	1.3				
		50–52	29					17	1.2				
		60–62	27					19	1.2				
		70–72	27					20	1.1				
		80–82	23					21	1.1				
		90–92	33					25	1.1				
		98–100	35						1.0				
16b	58	0–2	43	4890 ± 60	3687 ± 55	PTA 6945		53	0.8				
		10–12	38	7730 ± 90	6516 ± 79	Ki-10408	1	37	0.8	0.95	0.23	–1.16	0.10
		18–20	37	8990 ± 80	8007 ± 54	PTA 6941	2	29	0.9	1.11	0.26	–1.1	0.09
				8300 ± 80**	7356 ± 117	PTA 7412							
		20–22	40					29	1.0				
		30–32	47					35	1.0				
		40–42	37	11020 ± 80	10 982 ± 76	Ki-10409	4	21	1.2				
		50–52	41						1.1				
51b	35	0–2	30	11310 ± 130	11 264 ± 132	PTA 6946		22	1.3				
		10–12	29					22	1.1				
		20–22	27					23	1.3				
		30–32	27	8860 ± 90	7870 ± 121	PTA 6905	3	22	1.1				
		40–42	26					24	1.2				
		50–52	34	9530 ± 80	8679 ± 177	PTA 6930	5	26	1.2				
		60–62	25					24	1.1				
		70–72	27	10 520 ± 90	10 489 ± 104	PTA 6933	7	25	1.2				

				10 400 ± 90	10 329 ± 125	Ki-10410						
		80–82	27	10 540 ± 90	10 504 ± 102	Ki-10520	8	23	1.1			
		90–92	20	10 810 ± 110	10 782 ± 106	PTA 6902	8	24	1.2			
		100–102	25	10 450 ± 80	10 401 ± 101	Ki-10411		23	1.4			
		110–112	21	11 430 ± 100	11 388 ± 106	PTA 6935	10	23	1.3			
		120–122	25					21	1.2			
		130–132	25					21	1.2			
		140–142	23	12 080 ± 100	12 139 ± 123	PTA 6910	12	22	1.1			
80b	61.5	0–2	34	7750 ± 70	6523 ± 60	PTA 6887	0	23	1.1			
				7570 ± 90	6354 ± 92	Ki-10412						
		10–12	29					24	1.2			
		20–22	30					24	0.2			
		30–32	38	8980 ± 90	8003 ± 62	Ki-10413	3	24	1.1			
		40–42	39	11 310 ± 100	11 263 ± 102	PTA 6888	4	21	0.9			
		50–52	36					21	0.9			
		60–62	37					22	0.9			
		70–72	38					20	1.0			
		80–82	39					21	0.9			
		90–92	36					21	0.9			
		100–102	35					23	1.1			
		110–112	38					25	1.0			
		120–122	32	12 170 ± 110	12 250 ± 139	PTA 6891	10	23	1.0			
138b	80	0–2	46	7570 ± 60	6392 ± 66	PTA 6911	0	35	2.4	0.83	–0.55	–0.88	0.37
		10–12	43					32	1.0				
		20–22	42					27	1.0				
		30–32	46	9080 ± 90	8092 ± 88	PTA 6912	3	26	0.8	0.76	–0.48	–0.9	0.49
				9790 ± 80	9070 ± 82	Ki-10415							
		40–42	45					27	0.8				
		50–52	37	13 370 ± 100	N/A	Ki-10417	4	25	0.9				
		60–62	40	13 500 ± 140	N/A	PTA 6913	4	24	0.9				
		70–72	40						0.9				

Source: From previously unpublished data of the authors.

Notes: Ki—Kiev Radiocarbon Laboratory, Kiev, Ukraine; PTA—Quaternary Dating Research Unit, CSIRO, Pretoria, South Africa.

*Coordinates of the stations are given in Koral et al. (2001).

**^{14}C on corals from Koral et al. (2001).

(Perinçek and Çemen, 1990; Aksu et al., 1992; Kempler, 1994). The latter moves northward underneath the Eurasian plate along the Bitlis-Zagros suture and pushes the Anatolian plate westward along the Eastern Anatolian fault and the Dead Sea fault zone (Şengör and Yılmaz, 1981; Şengör et al., 1985; Robertson, 1998), causing intensive faulting in the Quaternary succession (Perinçek and Çemen, 1990; Aksu et al., 1992; Kempler, 1994).

MATERIALS AND METHODS

Data Collection and Bathymetry

Data for this study were collected by the AVICENNE international project in the spring of 1993 (AVI-2) and the winter of 1995 (AVI-4; AVICENNE Annual Report, 1993, 1995, 1996; Basso et al., 1994; Yanko et al., 1998; Basso and Spezzaferri, 2000). The AVI-2 cruise obtained 142 grab samples and two gravity cores with the Turkish research vessel *Koca Piri Reis* at water depths from 3 to 85 m. The AVI-4 cruise repeated sampling at the same stations and recovered five more gravity cores. The cores were split in two parts. The working half of the cores was divided into 10 cm intervals. Fifty-four sediment samples were collected from the uppermost 2 cm of each interval, 142 samples from the surface of the grab samples. Each sample was subdivided for lithological, geochemical, isotopic, and foraminiferal analyses. Twenty-seven samples were dated by ^{14}C (Table 1). Two cores are presented elsewhere by Spezzaferri et al. (2000), whereas five cores are described here.

The depth readings collected by the AVI-2 cruise were used to construct a detailed (10-m interval isobath) bathymetric map of Iskenderun Bay (Fig. 1A) to discern the bottom morphology.

Lithology

Grain size analysis was performed at Istanbul University, Turkey. The sediments were divided into clay (<0.0039 mm), silt (0.0039–0.0625 mm), sand (0.0625–2.0 mm), and gravel (>2 mm) fractions. The methods used included wet sieving for the sediment with grain size greater than 63 μm and pipette analyses for clay and silt fractions, as described in Folk (1974).

Grain size data were utilized to identify the lithotypes (Table 2). A lithotype is a geological unit characterized by its specific lithological features, mode, and conditions of sediment deposition (Frolov, 1995; Motnenko, 1999) and is named after the dominant and secondary fraction. For example, the sediment sample from St. 1 contains 67% silt and 18% clay. Consequently, it is referred to as clayey silt or STcl. The lithotypes with $CaCO_3$ exceeding 50% have the ending "Bio." For example, the sediment sample from St. 21 contains 78% of $CaCO_3$ and is referred to as SAstBio. In this work, we call ST, STsa, STcl, CL, CLsa, and CLst lithotypes fine-grained sediments to distinguish them from coarse-grained sediments (lithotypes GR, GRsa, SA, SAst, and SAcl). The lithotypes are plotted on a bathymetrical map to assist in visualizing the geomorphology of the bay floor (Fig. 2).

Carbonate Content and Organic Carbon

In the cores (Table 1) and surface (Table 2) samples, the total carbonate content (expressed as the percent $CaCO_3$) of the sediment was measured by volumetric Ca analysis (Grillot et al., 1964). In the core samples, C_{org} (Table 2) was measured by oxidation of organic matter by dichromate solution. During oxidation, the reddish Cr^{+6} was reduced to greenish Cr^{+3}, measured with a colorimeter, and calculated by a standard curve (Schlichting and Blume, 1966).

Foraminifera

Live (Rose Bengal stained) and fossil benthic foraminifera were investigated separately as described by Yanko and Troitskaya (1987), Yanko (1989), and Yanko et al. (1998). Samples were soaked and washed in distilled water through a 63-μm mesh sieve. Live foraminifera were counted in wet samples equal to 5 g of dry sediment mass. The amount of wet sediment needed was calculated by means of the water content at each station. The two dominant species, with the highest abundance and occurrence among all other species, were plotted as a percentage of the total number of benthic species in each geomorphological element (Fig. 3).

Fossil foraminifera were studied in samples that were dried at room temperature to avoid destruction of agglutinated species; no flotation techniques were employed. Dried samples were split with a microsplitter to avoid sample bias, and about three hundred fossil foraminifera were picked by hand and counted for population statistics. The total number of benthic and planktonic foraminifera was calculated separately per 5 g dry sediment and the planktonic/benthic (P/B) ratio was plotted at selected horizons downcore (Figs. 4A–8A). Diagrams of the percentages of the four most abundant species as well as the remaining species are plotted to show the difference between the live and fossil foraminiferal assemblages in the top-core samples as well as downcore, including at the Holocene-Pleistocene boundary (Figs. 4B, C, and D through 8B, C, and D).

The taxonomic identification of foraminifera was carried out by direct comparison with the collection of eastern Mediterranean foraminifera obtained by the AVICENNE project and stored at the Avalon Institute of Applied Science, Canada. The original collections of d'Orbigny, Schlumberger, and Le Calvez in the Museum of Natural History, Paris, and published data (e.g., Cimerman and Langer, 1991; Hottinger et al., 1993; Sgarella and Moncharmont Zei, 1993) were used as well. The classification of Loeblich and Tappan (1988) was used to identify the foraminifera to the generic level. The collection of foraminifera from the core samples is stored at the Department of Geological Engineering, Çukurova University, Turkey. A

TABLE 2. GRAIN SIZE, $CaCO_3$ CONTENT, AND LITHOTYPES OF SURFACE SEDIMENTS IN ISKENDERUN BAY

Station	Water depth (m)	Gravel (%)	Sand (%)	Silt (%)	Clay (%)	$CaCO_3$ (%) AVI-2	$CaCO_3$ (%) AVI-4	Abbreviations for lithotypes listed below
1	18	0	15	67	18	11		STcl
2	53	10	21	68	0	n.d.		STsa
3	51	0	18	81	1	18		STsa
4	19	0	74	26	0	19		SAst
5	27	0	14	69	18	19		STcl
6	47	0	1	69	29	14		STcl
7	10	100	0	0	0	18		GR
8	7	0	61	35	3	15		SAst
9	31	0	10	62	28	15		STcl
10	9.5	0	88	10	3	21		SAst
11	56	0	1	98	0	16		ST
12a	42	0	3	97	0	26		ST
12b	42	0	11	89	0	21		STsa
13	32	0	15	85	0	n.d.		STsa
14	8	0	88	6	6	23		SAcl
15		100	0	0	0	n.d.	n.d.	GR
16a	58	0	4	96	0	n.d.	31	ST
16b	58	0	68	32	0		53	SAstBio
17	43	4	35	54	7	n.d.	53	STsaBio
18	32	18	41	41	0	n.d.	63	SAstBio
19	23	37	43	12	9	n.d.	21	SAgr
20	13	100	0	0	0	n.d.	19	GR
21	10	4	69	24	4	78		SAstBio
22	8	0	81	17	1	21		SAst
23	8	0	81	19	0	27		SAst
24	15	25	70	4	0	80		SAgrBio
25	17	26	69	5	0	85		SAgrBio
26	16	0	89	7	4	87		SAstBio
27	23	16	50	33	1	59		SAstBio
28	29	6	49	43	2	77		SAstBio
29	39	14	40	28	18	62		SAstBio
30	46	15	25	60	0	53		SAstBio
31	40	1	8	53	38	27		STcl
32	27	22	26	45	7	98		STsaBio
33	18	30	28	36	5	85		STGRBio
34	6	0	84	10	6	22		SA
35	14	0	2	98	0	n.d.	7	ST
36	20	0	53	47	0	69		SAstBio
37	37	1	11	76	12	32		STcl
38	41	0	3	97	0	25		ST
39	22	3	34	57	7	22		STsa
40	17	0	1	68	30	n.d.	28	STcl
41		100	0	0	0	n.d.	n.d.	GR
42	8	0	85	13	2	14		SAst
43	24	0	4	96	0	16		ST
44	42	0	2	94	5	18		ST
45	46	0	1	99	0	20		ST
45-A	38	0	35	45	19	16		STsa
46	20	0	16	76	8	18		STsa
47	8	0	49	51	0	n.d.	20	STsa
48	8	3	85	12	0	20		SAst
49	10	0	69	31	0	n.d.	26	SAst
50	23	0	3	97	0	20		ST
51a	35	0	3	73	24	n.d.	21	STcl
51b	35	0	3	97	0		22	ST
52	21	0	21	79	0	24		STsa
53	18	0	5	95	0	29		ST

(*continued*)

TABLE 2. *Continued*

Station	Water depth (m)	Gravel (%)	Sand (%)	Silt (%)	Clay (%)	$CaCO_3$ (%) AVI-2	$CaCO_3$ (%) AVI-4	Abbreviations for lithotypes listed below
54	8	0	88	11	0	39		SAst
55		100	0	0	0	n.d.	n.d.	GR
56	11	0	32	11	56	n.d.	n.d.	Clsa
57	9	0	85	6	9	n.d.	n.d.	SAcl
58		100	0	0	0	n.d.	n.d.	GR
59	8	1	94	5	0	33		SA
60	18	0	68	27	6	29		SAst
61	42	0	1	99	0	19		ST
62	41	0	1	99	0	n.d.	21	ST
63	43	0	3	95	2	20		ST
64	47	0	1	99	0	n.d.	23	ST
65	51	0	1	95	5	20		ST
66	54	0	1	99	0	23		ST
67	49	0	4	93	3	28		ST
68	60	100	0	0	0	n.d.	22	GR
69	60	0	5	61	33	22		STcl
70	68	2	7	75	16	20		STcl
71	68	0	1	99	0	19		ST
72	63	0	1	54	45	19		STcl
73	57	0	10	76	14	8		STcl
74	41	0	5	46	50	20		STcl
75	9	0	43	57	0	31		STsa
76	10	0	54	46	0	26		SAst
77	21	0	60	40	0	25		SAst
78	41	0	1	75	24	1		STcl
79	56	0	52	31	17	28		SAst
80a	61	1	50	49	0	29		SAst
80b	62	0	5	95	0	23		ST
81	70	0	1	99	0	20		ST
82	70	0	1	54	45	15		STcl
83	37	0	5	60	35	38		STcl
84	11	2	63	26	9	15		SAst
85	13	0	82	17	0	11		SAst
86	71	0	1	98	0	19		ST
87	72	0	3	97	0	2		ST
88	68	100	0	0	0	20		GR
89	63	0	4	96	0	20		ST
90	48	0	1	65	34	19		STcl
91	44	0	1	99	0	20		ST
92	23	0	62	38	0	39		SAst
93	11	0	72	28	0	n.d.	33	SAst
94	12	0	50	49	0	26		SAst
95	22	0	31	69	0	43		STsa
96	21	0	27	35	38	20		STcl
97	55	0	5	96	0	20		ST
98	69	0	1	69	30	21		STcl
99	73	0	0	53	47	14		STcl
100	76	1	2	58	39	19		STcl
101	63	5	13	58	24	28		STcl
102	11	0	76	24	0	36		SAst
103	12	12	49	26	14	47		SAst
104	55	3	13	50	33	32		STcl
105	78	7	4	89	0	15		ST
106	76	1	6	93	0	20		ST
107	72	0	5	89	6	19		ST
108	61	0	0	68	32	20		STcl
109	24	0	3	97	0	19		ST
110	13	0	7	45	48	n.d.	24	STcl
111	54	0	1	99	0	21		ST
112	75	0	4	52	44	18		STcl

TABLE 2. *Continued*

Station	Water depth (m)	Gravel (%)	Sand (%)	Silt (%)	Clay (%)	$CaCO_3$ (%) AVI-2	$CaCO_3$ (%) AVI-4	Abbreviations for lithotypes listed below
113	70	0	2	98	0	18		ST
114	82	0	1	38	61	n.d.	26	STcl
115	52	11	51	31	6	67		SAstBio
115-A	55	14	18	67	0	n.d.	n.d.	STsa
116	40	16	27	56	1	62		STsaBio
117	30	13	63	24	0	n.d.	51	SAst
118	15	1	60	36	3	11		SAst
119	16	0	94	4	2	21		SA
120	7	100	0	0	0	n.d.	86	GRBio
121	23	10	77	13	0	63		SAstBio
122	43	32	32	21	15	60		GRsaBio
123	21	9	87	3	0	52		SAGRBio
124	15	0	8	92	0	4		STsa
125	24	100	0	0	0	n.d.	17	GR
126	49	17	15	68	0	50		STGRBio
127	65	3	16	79	3	8		STsa
128	82	0	2	63	35	23		STcl
129	80	0	1	99	0	17		ST
130	76	0	0	100	0	18		ST
131	44	0	0	0	100	20		CL
132	19	0	12	74	14	14		STcl
133	11	0	16	16	68	1		CLsa
133-A	22	0	13	66	22	25		STcl
134	61	0	4	79	17	20		STcl
135	76	0	6	94	0	17		ST
136	82	0	3	92	5	15		ST
137	85	0	1	82	17	27		STcl
138a	79	2	10	62	26	30		STcl
138b	80	0	15	85	0	35		ST
139	12	0	12	88	0	3		STsa

Source: From previously unpublished data of the authors.

Notes: Lithotype abbreviations: Bio—biogenic; CLsa—sandy clay; GR—gravel; GRsa—sandy gravel; n.d.—not detected; SA—sand; SAcl—clayey sand; SAgr—gravely sand; SAst—silty sand; STsa—sandy silt; ST—silt; STcl—clayey silt.

complete taxonomic list of foraminifera and their quantitative distribution in the samples is presented in an appendix that appears elsewhere.[1]

Oxygen and Carbon Isotopes

To explore the general paleoceanographic characteristics of the bay, oxygen and carbon isotopes were measured in fifty tests of the planktonic species *Globigerinoides ruber* (d'Orbigny) and the benthic species *Porosononion martkobi* (Bogdanowich) (Table 1). The analysis was performed in the Stanley Margolis Stable Isotope Laboratory at the Department of Geology, University of California, Davis. Foraminiferal tests were roasted in a vacuum for 60 min at 375 °C to remove any volatile organic carbon. Using a common bath autocarbonate device peripheral to the mass spectrometer, each sample was reacted at 90 °C in 103% phosphoric acid. The resultant CO_2 was purified for any water and analyzed by comparison with the CO_2 generated from NBS-19. Isotopic analysis was done with a Micromass Optima Isotope Ratio Mass Spectrometer, and the analytical precision was ± 0.06 per mil for ^{18}O and ± 0.05 per mil for ^{13}C analyses. Isotope ratios of ^{13}C and ^{18}O were calculated relative to the Vienna-PDB (VPDB) standard.

Radiocarbon Dating

Radiocarbon dating was performed at the Quaternary Dating Research Unit, Pretoria, South Africa, and at the Kiev Radiocarbon Laboratory, Kiev, Ukraine (Table 1). For the ^{14}C analysis, bulk carbonate (consistently 30% of the sediment) from 2-cm slices of the cores was dried, microscopically analyzed, and treated with hydrochloric acid to decompose the carbonate, and the released carbon dioxide was used for radiometric analy-

[1]GSA Data Repository item 2006186, Appendix of foraminiferal data, is available online at www.geosociety.org/pubs/ft2006.htm, or on request from editing@geosociety.org or Documents Secretary, GSA, P.O. Box 9140, Boulder, CO 80301, USA.

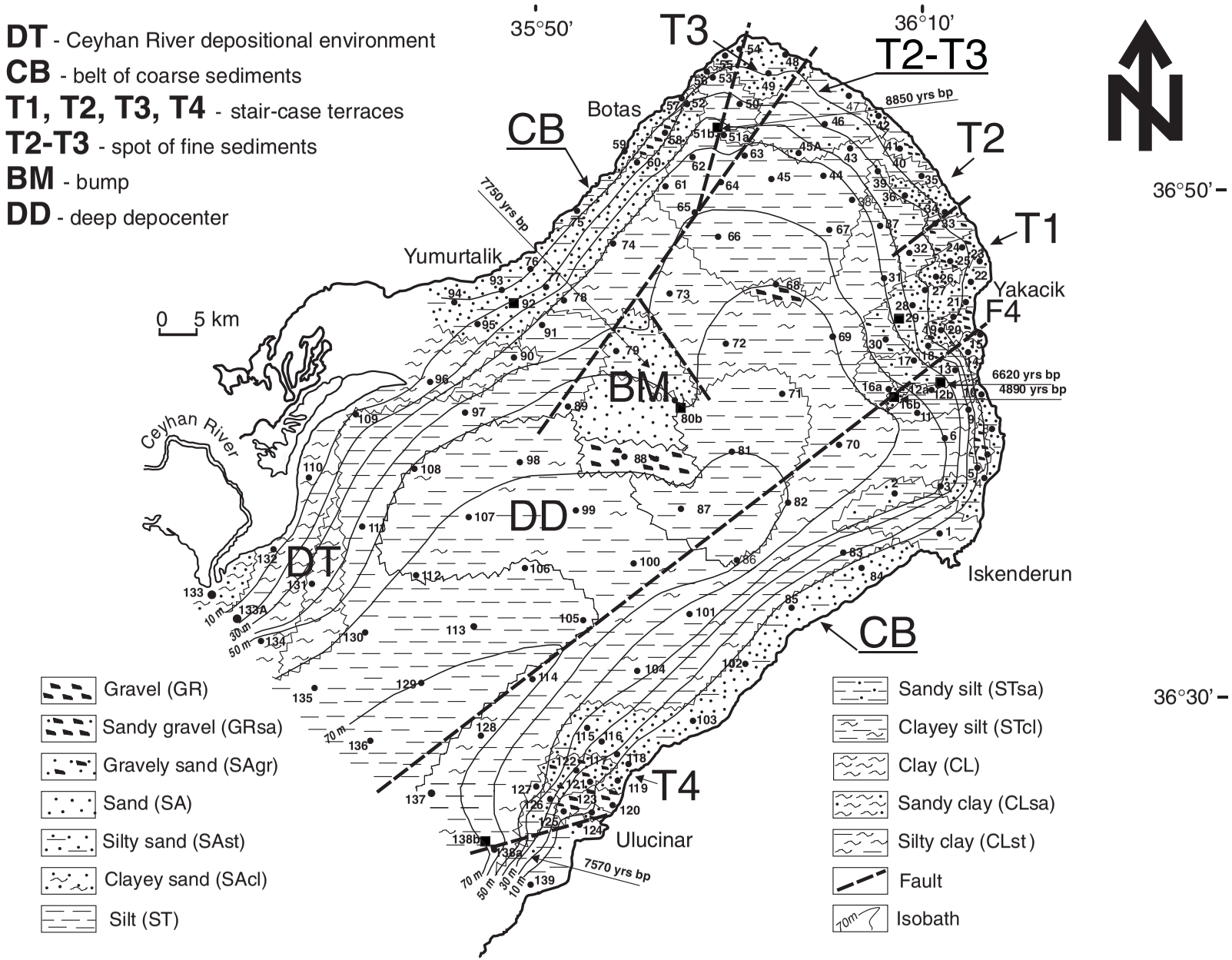

Figure 2. Lithological map of Iskenderun Bay showing the bathymetrical distribution of lithotypes, stair-case tectonic structures, and faults.

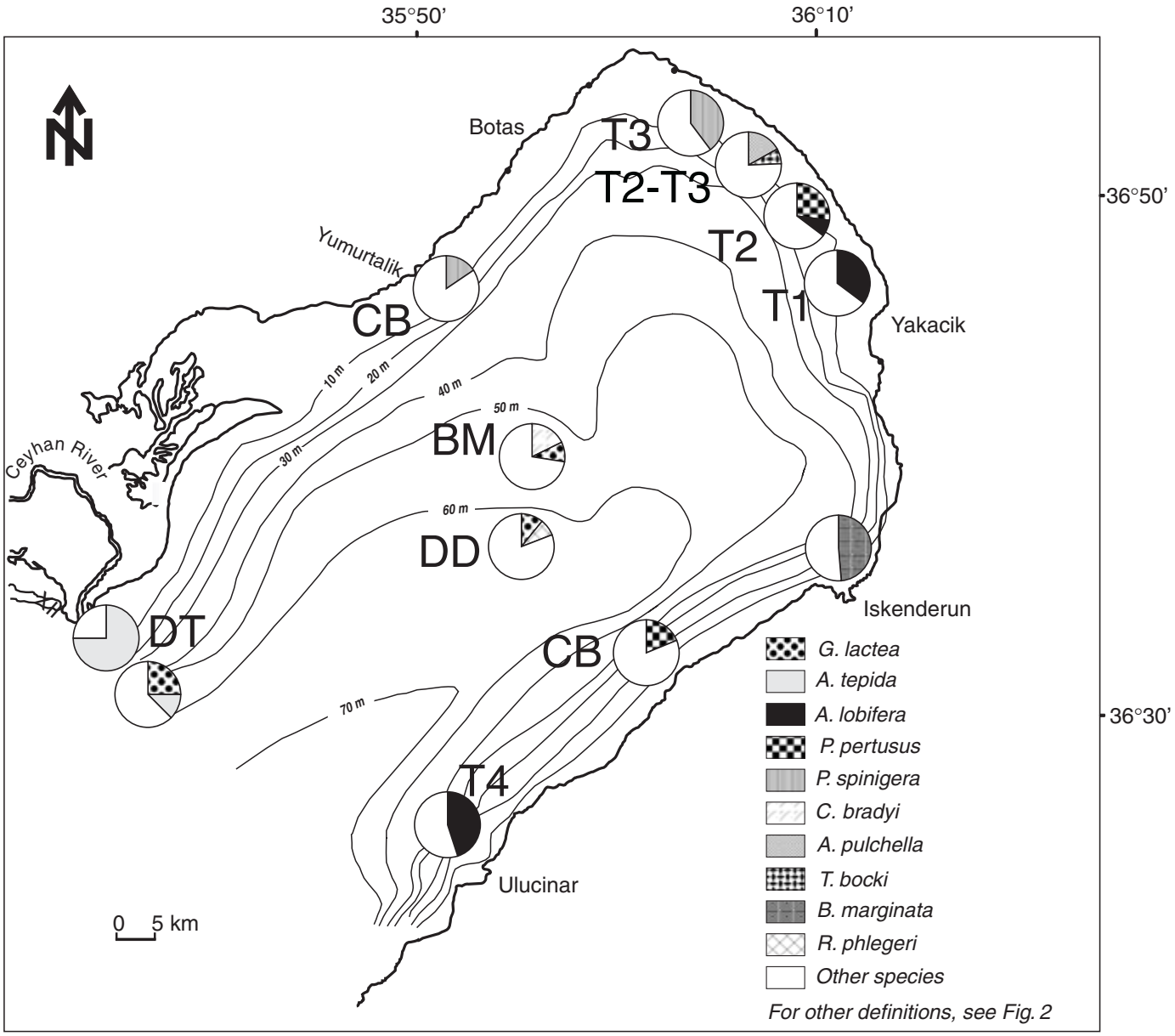

Figure 3. Diagrams showing the percentage of dominant and accessory species in Rose Bengal stained foraminiferal assemblages of the depositional environments indicated on the bathymetrical map. The gray and black colors indicate the percentages of *Ammonia tepida* and *Amphistegina lobifera,* respectively. The former is an indicator of a shallow environment affected by freshwater input, the latter of hard ground or reeflike substrate.

sis in a gas proportional counter (Vogel and Marais, 1971; Skripkin et al., 1994; Skripkin and Kovalyukh, 1998). Microscopic analysis revealed that the bulk carbonate consists mainly of foraminifera, coral rodlets, and detritus of mollusk shells. In core 16, however, the coral rodlets found in their original position (PTA7412) were removed from the sediments before analysis to be analyzed separate from the bulk carbonate (PTA 6941).

The ^{14}C data have been calibrated with the Groningen Radiocarbon Calibration Program CAL25 (Van Der Plicht, 1993) using the technique described by Bernhard Weninger (1986). The reservoir age of the Mediterranean water (e.g., 254 ± 50 yr, obtained on *Chlamys varia* [Linne] at site 493, Beirut, Lebanon, closest to Iskenderun Bay; Reimer and McCormac, 2002) could not be used for calibration because (1) recent

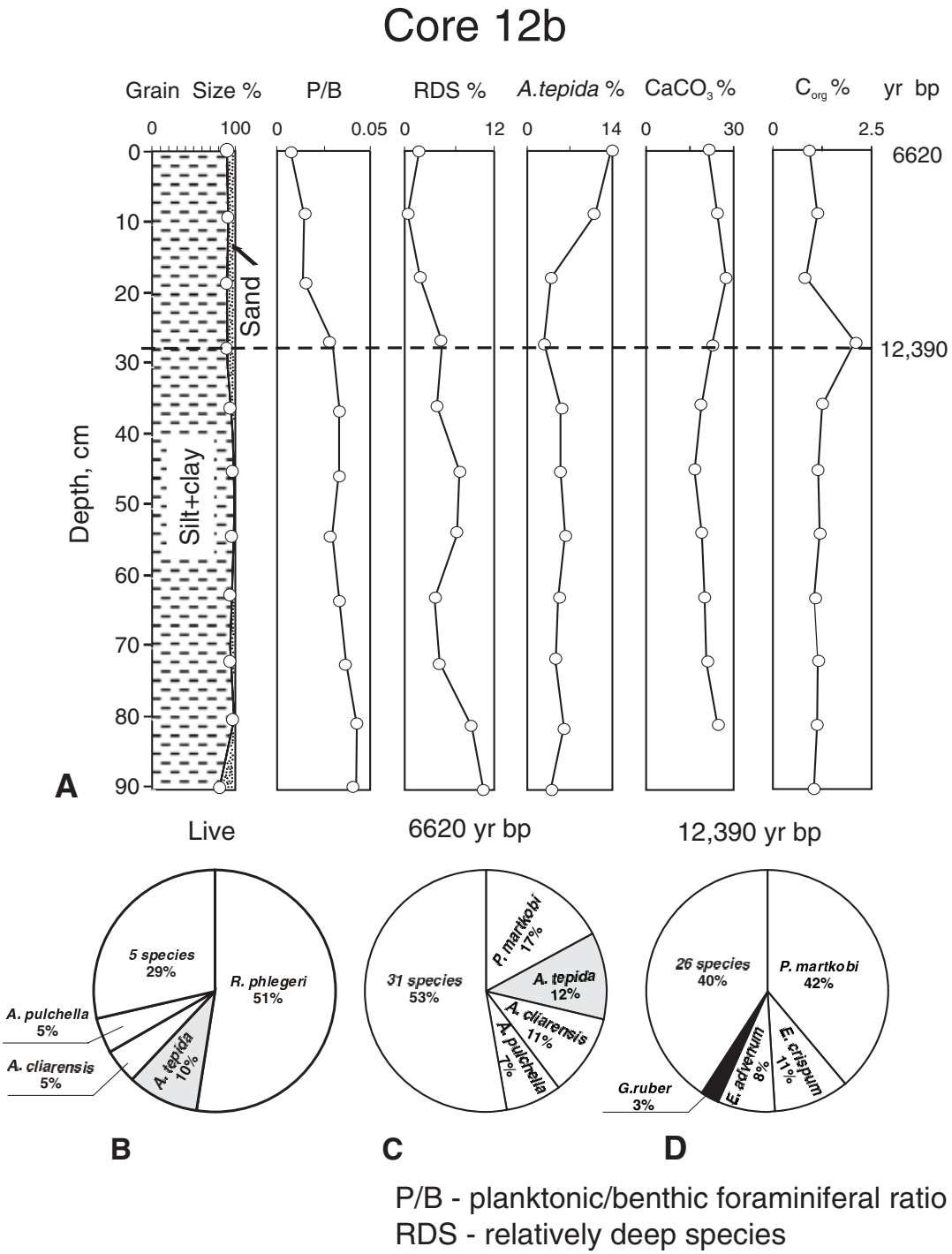

Figure 4. Core 12b: The dotted line indicates the Early Holocene-Late Pleistocene boundary. (A) Distribution of grain size, P/B, RDS, *A. tepida,* $CaCO_3$, and C_{org} in the sedimentological column; (B–D) diagrams showing dominant and accessory foraminiferal species in the (B) live (Rose Bengal stained) assemblage; (C) core-top Holocene (6620 yr bp) assemblage; (D) late Pleistocene (12,390 yr bp) assemblage (*G. ruber* and *A. tepida* in black and gray, respectively).

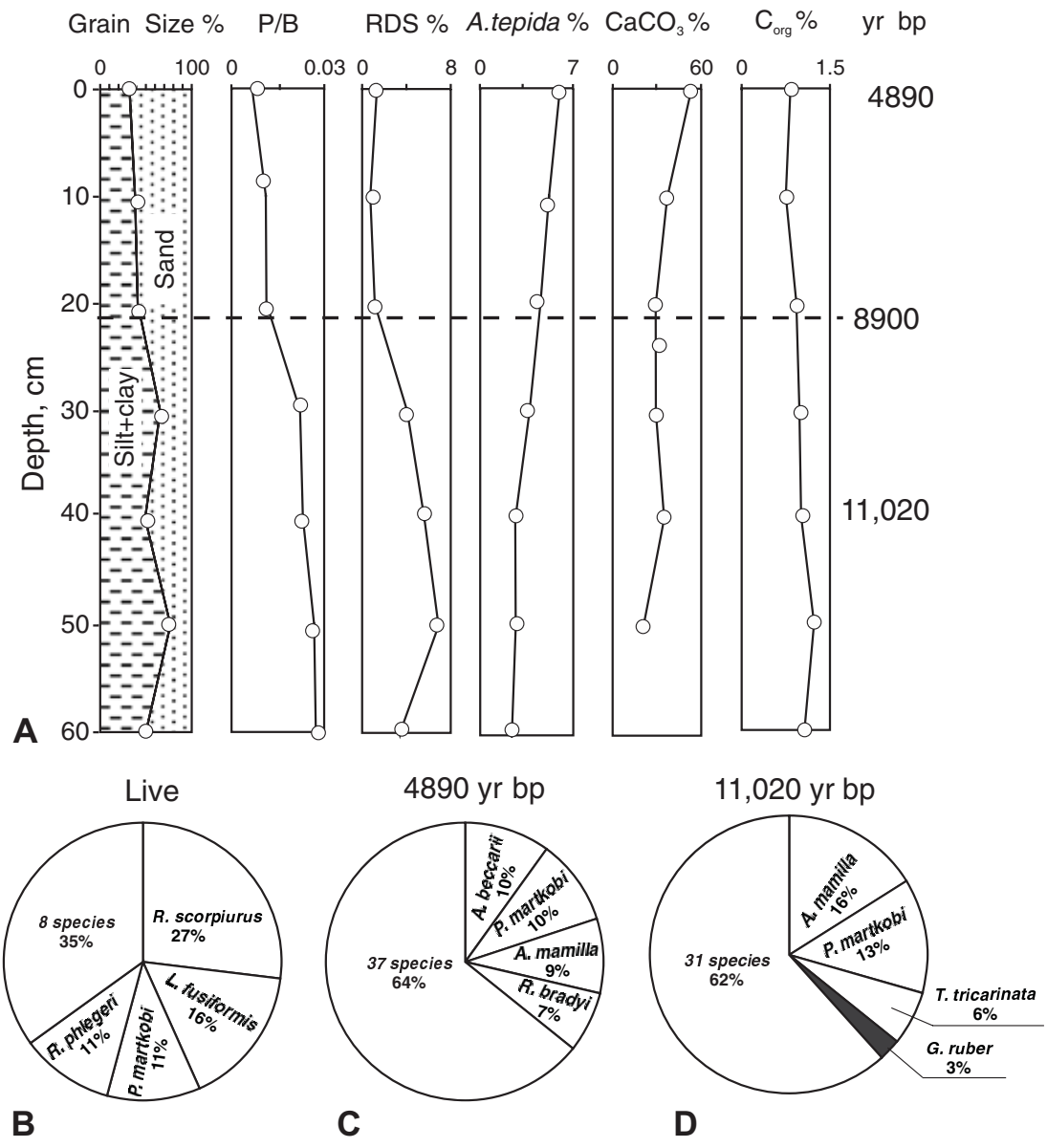

Figure 5. Core 16b: The dotted line indicates the Holocene-Pleistocene boundary. (A) Distribution of grain size, P/B, RDS, *A. tepida,* $CaCO_3$, and C_{org} in the sedimentological column; (B–D) diagrams showing dominant and accessory foraminiferal species in the (B) live (Rose Bengal stained) assemblage; (C) core-top Holocene (4890 yr bp) assemblage; (D) late Pleistocene (11,020 yr bp) assemblage (*G. ruber* in black).

Core 51b

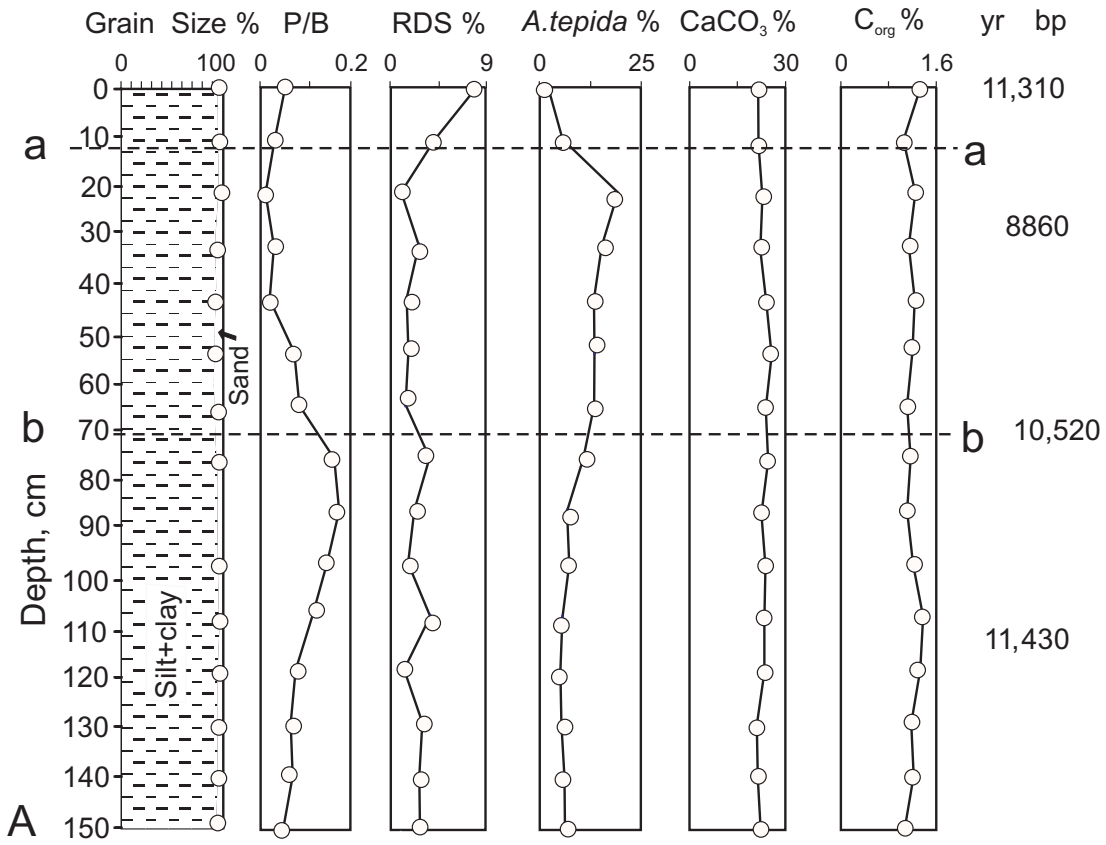

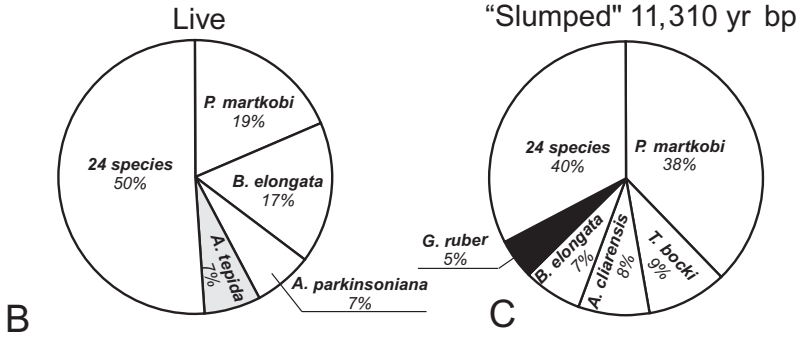

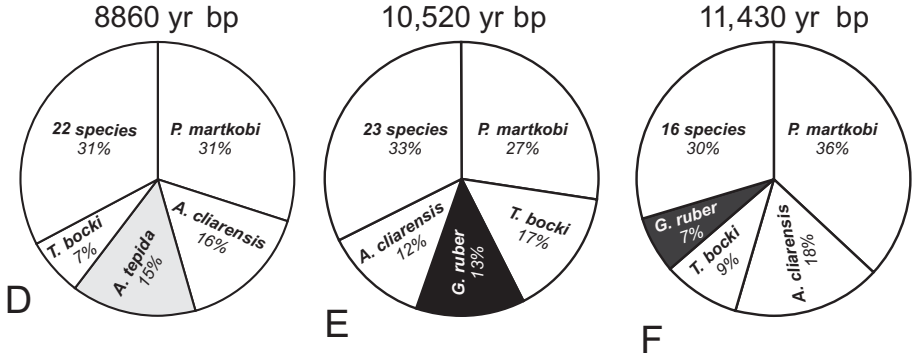

P/B - planktonic/benthic foraminiferal ra
RDS - relatively deep species

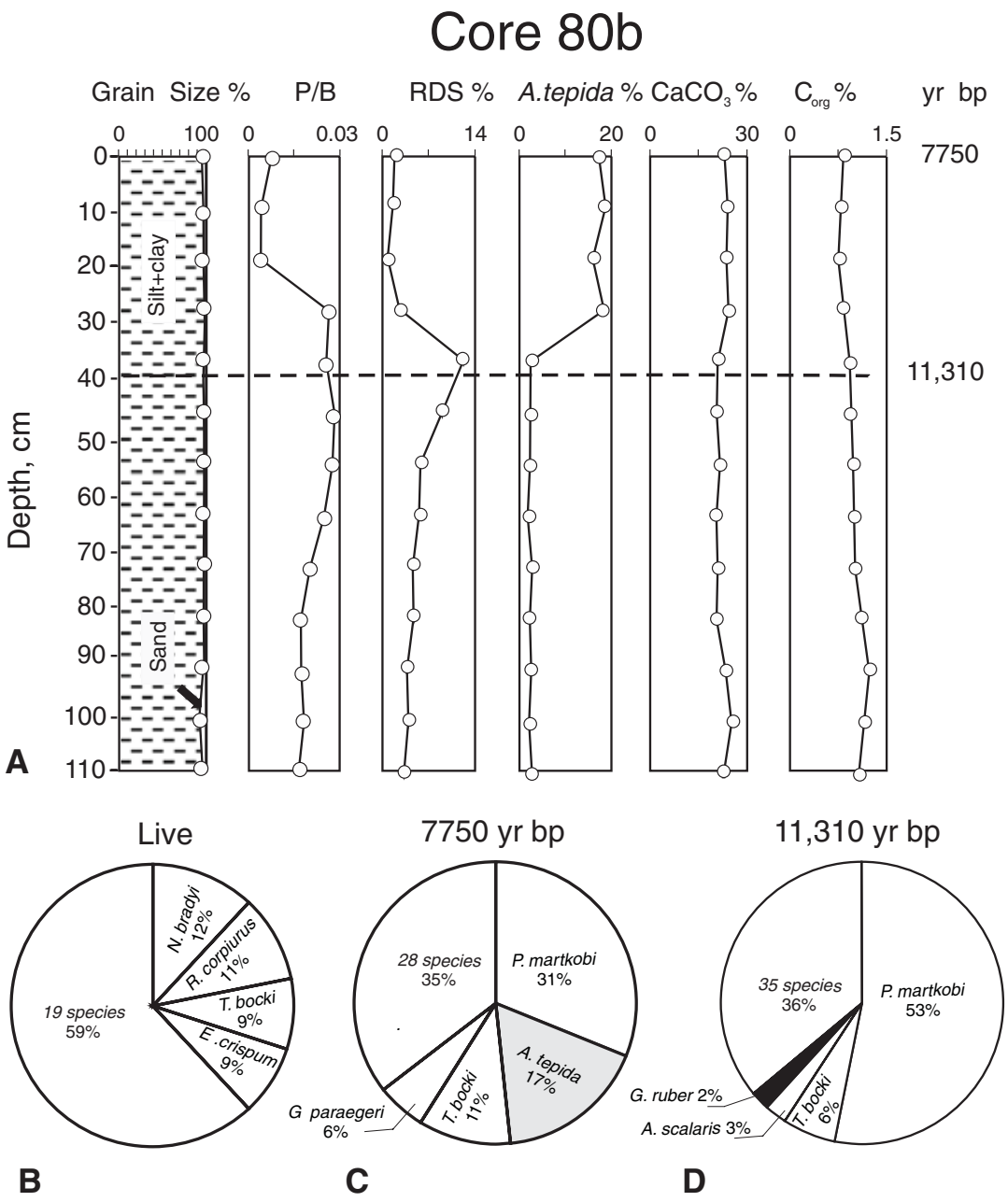

Figure 7. Core 80b: The dotted line indicates the Holocene-Pleistocene boundary. (A) distribution of grain size, P/B, RDS, *A. tepida,* $CaCO_3$, and C_{org} in the sedimentological column; (B–D) diagrams showing dominant and accessory foraminiferal species in the (B) live (Rose Bengal stained) assemblage; (C) core-top Holocene (7750 yr bp) assemblage; (D) late Pleistocene (11,310 yr bp) assemblage.

Figure 6. Core 51b: The dashed line a-a indicates the boundary between "slumped" late Pleistocene and in situ Holocene samples. The dashed line b-b indicates the Holocene-Pleistocene boundary. (A) Distribution of grain size, P/B, RDS, *A. tepida,* $CaCO_3$, and C_{org} in the sedimentological column; (B–E) diagrams showing dominant and accessory foraminiferal species in the (B) live (Rose Bengal stained) assemblage; (C) core-top "slumped" late Pleistocene (11,310 yr bp) assemblage, which is similar to the (F) late Pleistocene (11,430 yr bp) assemblage; (D) Holocene (8860 yr bp) assemblage. (E) Late Pleistocene (10,520 yr bp) assemblage.

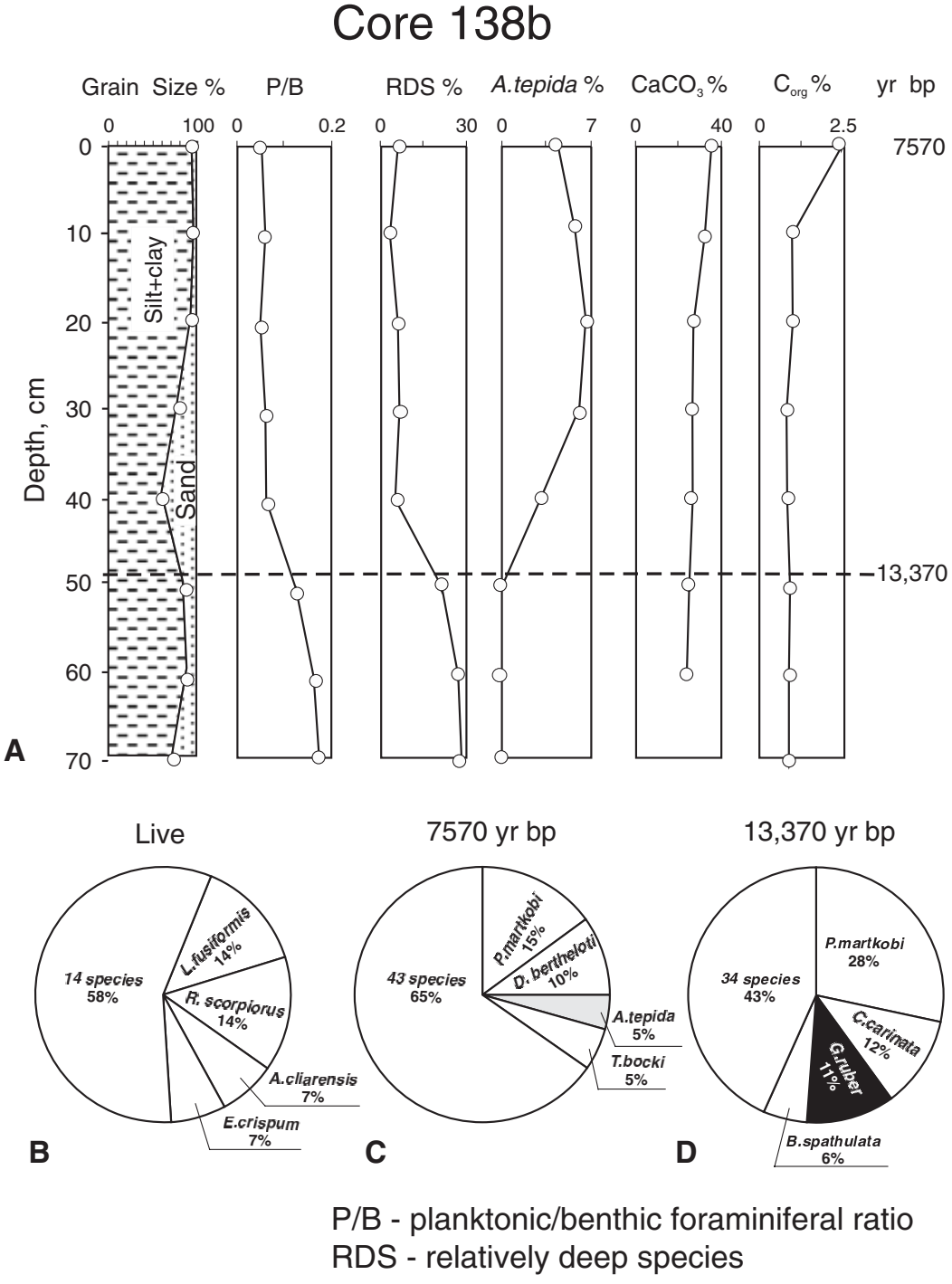

Figure 8. Core 138b: The dotted line indicates the Holocene-Pleistocene boundary. (A) Distribution of grain size, P/B, RDS, *A. tepida,* $CaCO_3$, and C_{org} in the sedimentological column; (B–D) diagrams showing dominant and accessory foraminiferal species in the (B) live (Rose Bengal stained) assemblage; (C) core-top Holocene (7570 yr bp) assemblage; (D) late Pleistocene (13,370 yr bp) assemblage.

^{14}C datings of mollusks' shells show a highly variable Mediterranean Sea reservoir age (Pelc, 1995); (2) coastal waters may contain "old carbon" supplied by rivers and thus may have a larger reservoir effect than open-ocean waters. Because of this uncertainty, the reservoir age of surface ocean water, ~400 yr, was subtracted from all the radiocarbon dates for calibration. The abbreviation bp (lowercase) is used for uncorrected dates, BP (uppercase) for calibrated dates. Throughout the text, ^{14}C data are expressed as uncorrected years bp to be comparable with worldwide Pleistocene or Holocene chronology and sea level curves (e.g., Fairbanks, 1989).

RESULTS

Oceanography or Paleoceanography

The main oceanographic parameters of Iskenderun Bay are presented in AVICENNE Annual Report (1995, 1996) and discussed by Basso et al. (1994) and Basso and Spezzaferri (2000). The bottom salinity is rather uniform (the median value is 39.1‰). Even at the outlet of the Ceyhan River (St. 133, depth –11 m), the median salinity does not change significantly; it is 38.6‰ and 39.1‰ in spring and winter, respectively. Today, there is less than 2‰ difference in the surface and bottom salinity as documented by spring measurements.

Sea Bottom Morphology, Lithology, $CaCO_3$, ^{14}C, and Foraminifera

The bottom of the bay has a stair-case morphology that is especially notable on the northern flank (Fig. 1A and F). The southeast flank is narrower and steeper than the northwest flank (Fig. 1A–F). Based on bathymetrical profiles (because of lack of seismic evidence), there are "bumps" up to 30 m in height above the surrounding bottom morphology on each side (Fig. 1B and F) and in the center (Figs. 1A, B, and L) of the bay. There is a tilting of the floor to the southeast (Fig. 1M) and then to the northwest (Fig. 1Q) at a depth of ~70 m. Along the principal axis, the bay gradually deepens toward the Mediterranean Sea (Fig. 1D and E).

The following geomorphological elements are distinguished clockwise along the shore from the bathymetrical and sedimentological data (Fig. 2): the Ceyhan River delta (DT), the belt of coarse sediments (CB), stair-case terraces (T1, T2, T3, and T4), and a depression between the T2 and T3 terraces (T2-T3). The central part of the bay is represented by a deep depocenter (DD), and there is a bump (BM) in the middle of DD (Fig. 2).

The Ceyhan River pro-delta (DT) is adjacent to the Ceyhan River mouth and encompasses St. 96, 109, 110, 131, 132, 133, 133A, and 134, where the finest lithotypes, CL, CLsa, and CLst (average $CaCO_3$ 18%), have accumulated at a depth of 11–61 m. In front of the river mouth, the grain size distribution grades outward, but is sharply truncated in a northwest orientation. In the shallow part of the delta (St. 133, depth 11 m), the foraminiferal assemblage contains two species, with *A. tepida* (75%) dominant. Toward the sea (St. 134, depth 61 m), *Guttulina lactea* (Walker and Jacob) and *Rectuvigerina phlegeri* (Le Calvez), both silt-clay dwellers (Sgarella and Moncharmont Zei, 1993), assume a dominant role (Fig. 3).

The belt of coarse sediment (CB) is distributed around the bay, starting from the town of Yumurtalik on the north and continuing clockwise to Ulucinar on the south. It is wider on the northeast than on the southeast slope, distributed to the 30 m and 10 m isobaths, respectively. There are stair-case terraces (Fig. 2) at the head of the bay (T1, T2, T3) and near its mouth on the southeast side (T4).

Stair-case terrace T1 (St. 16b, 17, 18, 19, 20, 21, 22, 23, 24, 25, 26, 27, 28, 29, and 30) lies in the northeast corner of the bay at depths of 8–58 m (average 25.4 m). It is covered by coarse biogenic (average $CaCO_3$ 60%) sediments (4890 yr bp, St. 16b) that locally pass to a "coralligenous" ("reeflike") bottom with multidecimetric concretions of coralline red algae, live coral *Cladocora caespitosa* (Linne) (e.g., St. 20), bivalve mollusks *Arca noae* (Linne) (Basso et al., 1994; Capitani et al., 2000), and foraminifera (58 species). The latter are frequently dominated by *Amphistegina lobifera* (Larsen) (Fig. 3).

Stair-case terrace T2 (St. 33, 34, and 36) is located to the northwest of T1 at shallower depths of 6–20 m (average 16.4 m). It is covered by high-carbonate (average $CaCO_3$ 59%) biogenic sediments, similar to those in T1. However, the abundance of *A. lobifera* sharply decreases, and *Peneroplis pertusus* (Forskal) becomes a dominant species in a relatively impoverished (26 species) foraminiferal assemblage (Fig. 3).

Stair-case terrace T3 (St. 48, 49, 54, and 55) is located to the north-northwest of T2 at water depths of 8–10 m (average 8.7 m). It is covered by coarse sediments with a much lower carbonate content (average $CaCO_3$ 28%) and number of foraminiferal species (18). The dominant species is *Pararotalia spinigera* (Le Calvez) (Fig. 3). There is a depression (T2-T3) between the T2 and T3 terraces (St. 45A, 46, and 47), with an average depth of 23 m. It is filled with low-carbonate (average $CaCO_3$ 17%), fine-grained sediments. The foraminiferal assemblage (26 species) is dominated by *Adelosina pulchella* d'Orbigny and is totally different from that of T2 and T3 (Fig. 3).

Stair-case terrace T4 (St. 115, 116, 117, 118, 119, 120, 121, 122, 123, 125, 126) is located on the east, with an average water depth of 29 m, $CaCO_3$ content of 49%, and a foraminiferal assemblage of 39 species that is dominated by *A. lobifera* (Fig. 3). Lithologically and microfaunistically, T1 and T4 are almost identical, but the sediments in T4 are nearly 2700 yr older (7570 yr bp, St. 138b).

The deep depocenter (DD) (St. 31, 38, 44, 45, 61, 62, 64, 65, 66, 67, 69, 70, 71, 72, 73, 74, 78, 81, 82, 86, 87, 90, 91, 97, 98, 99, 100, 101, 104, 105, 106, 107, 108, 111, 112, 113, 114, 128, 129, 130, 135, 136, 137, and 138a) has an average water depth of 60 m and comprises over 60% of the bay-fill (Fig. 2). It is covered by fine-grained sediments with relatively low carbonate content (average $CaCO_3$ 19.7%). The sediments are

dominated by the clay minerals smectite, halloysite, illite, and kaolinite, which were deposited from suspension in lower-energy environments by local terrestrial drainage (AVICENNE Annual Report, 1996). The foraminiferal assemblages (83 species) are dominated by *G. lactea, R. phlegeri* (Fig. 3), and accessories species *Textularia bocki* Hoglund and *Lagenammina fusiformis* (Williamson), all mud-clay dwellers that have a median depth distribution below 50 m (Basso and Spezzaferri, 2000).

The bump BM (St. 79, 80a, and 88) is an elevated area (a horst?) of ~150 km^2 at a depth of 55.7–68.1 m (average 61.5 m) in the center of the bay (Fig. 2) that is covered by coarse sediments (average $CaCO_3$ 26%). It is surrounded by fine sediments with an average $CaCO_3$ of 20%. The foraminiferal assemblage (19 species) is dominated by *Challengerella bradyi* (Billman, Hottinger, and Oesterle) (Fig. 3).

Core Lithology, $CaCO_3$, ^{14}C, and Foraminifera

The coarse fraction increases upward in cores 12b (Fig. 4A) and 16b (Fig. 5A), changes insignificantly in cores 51b (Fig. 6A) and 80b (Fig. 7A), and decreases upward in cores 138b (Fig. 8A). Thus, grain size data do not contribute much to our understanding of the depositional environment. The value of $CaCO_3$ decreases downward in cores 12b (Fig. 4A) and 16b (Fig. 5A) and is rather uniform in cores 51b (Fig. 6A), 80b (Fig. 7A), and 138 (Fig. 8A). The highest value of $CaCO_3$ (up to 53%) is in core 16b. In other cores, it varies between 17% and 35% (Table 1). The amount of C_{org} ranges between 0.2% and 2.4% (average 1.1%; Table 1; Figs. 4A–8A) and in general is larger than that in the surface sediments (0.3%–0.8%; average 0.6%), as reported by Ergin et al. (1996).

In total, live and fossil foraminifera in the cores are represented by 138 benthic and 1 planktonic (*G. ruber*) species. Thirty-five of the benthic species, as well as *G. ruber,* recovered from the cores do not live in Iskenderun Bay today. Among the 127 fossil species, 27 prefer circalittoral and bathyal environments. In this study, they are referred to as relatively deep species (RDS; Table 3). For example, in the Adriatic Sea, *Planulina ariminensis* d'Orbigny, *Angulogerina angulosa* (Williamson), *Brizalina spathulata* (Williamson), *Amphycorina scalaris* (Batsch), and *Bigenerina nodosaria* d'Orbigny have a strong tendency to occur in higher abundances with increasing water depth below 60 m (Jorissen, 1987); *A. angulosa* and *B. spathulata* have their highest frequencies at a depth of 146–400 m, whereas *B. nodosaria* occurs most frequently at a depth of 146–1000 m (Stigter et al., 1998). In the eastern Mediterranean, *A. angulosa, P. ariminensis, Globocassidulina subglobosa* (Brady), *B. nodosaria,* and *Biloculinella labiata* (Schlumberger) have their shallowest limit depth at 143 m (Parker, 1958), whereas *Lagenaminna fusiformis* (Williamson), *Bulimina aculeata* d'Orbigny and *Biloculinella inflata* (Wright) increase in abundance with depth (Basso and Spezzaferri, 2000). About 40% of RDS are absent in the live assemblages. Of the 35 species that do not live in Iskenderun Bay today, ~40% are represented by RDS. Distribution of those foraminiferal species and parameters (e.g., percentage of RDS and *A. tepida* in the benthic assemblages, as well as the P/B ratio) that are used for paleoenvironmental reconstructions is given in the appendix and plotted on Figures 4A–8A. In all cores, the percentage of RDS decreases synchronously with the P/B ratio, whereas the percentage of *A. tepida* increases upward.

Isotopic Composition

Oxygen and carbon isotopic data on foraminiferal tests vary (Table 1). The tests of the planktonic foraminifera are characterized by negative ^{18}O values ranging between –2.03‰ and –0.17‰, and the tests of the benthic foraminifera by positive values occurring are between 0.2‰ and 1.1‰. The ^{13}C value is positive for planktonic foraminifera and ranges between 0.88‰ and 1.75‰. It varies from negative (–0.06‰) to positive (0.61‰) values for the benthic foraminifera (Spezzaferri et al., 2003).

Radiocarbon Dating

Of the twenty-seven samples dated, the uncorrected ages range between 4,890 and 13,500 yr bp, whereas the ages calibrated using the method of Van Der Plicht (1993) fall between 3687 and 12,536 yr BP (Table 1). The radiocarbon ages exhibit only a small difference (~700 yr) between the coral rodlets and the enclosing bulk sample, and they increase consistently in a proper stratigraphical order down through all cores with the exception of core 51. In this core, the top sample (0–2 cm) has an older age (11,310 yr bp) than the underlying sample at 30–32 cm (8860 ± 90). The ages fall into two distinct groups: (1) "Holocene," from 4890 to 9790 yr bp, and (2) "Late Pleistocene," from 10,400 to 13,500 yr bp.

DISCUSSION

Geological Ages

The ^{14}C ages that were obtained at two different laboratories are of critical importance in many of the conclusions drawn in this article. It can be argued that the ^{14}C dates obtained from the bulk carbonate may represent composite ages (e.g., an average age for all of the organics in the sample), and therefore might not accurately represent the true age of the deposit (Puseman et al., 2001).

Depending on the number of factors that control the accumulation and decay of organic matter in a given deposit, the proportion of young to old carbon can be highly variable. As a result, large uncertainties in the measured ages may be inherent, making bulk ages questionable at best. Contamination of a bulk sample with younger carbon may have a greater effect on the resulting age than does contamination with older carbon (Polach et al., 1981; Rosholt et al., 1991). Studies by Andrews and Miller (1980) demonstrate that the addition of only 5% modern carbon

TABLE 3. WATER DEPTH DISTRIBUTION OF RELATIVELY DEEP SPECIES (RDS) FOUND IN THE CORES IN THE EASTERN AND WESTERN MEDITERRANEAN

		Eastern Mediterranean			Western Mediterranean	
			Median depth (m)			
No.	Species	Parker (1958)	Israeli shelf (AVI-1) AVICENNE Report (1995, 1996)	Iskenderun Bay (AVI-4; AVI-2) AVICENNE Report (1995, 1996), Basso and Spezzaferri (2000)	Gulf of Naples Sgarella and Moncharmont (1993)	Other areas Sgarella and Moncharmont (1993)**
1.	*Adelosina duthiersi**	Not found	47	79	22	Circalittoral
2.	*Adelosina partschii**	Not found	57	Not found	40	Not found
3.	*Amphicoryna scalaris*	Not found	192	82	60	Circalittoral, bathyal
4.	*Angulogerina angulosa*	143	200	69	?	Circalittoral, bathyal
5.	*Bigenerina nodosaria*	Not found	205	79	60	Circalittoral, bathyal
6.	*Biloculinella globula**	Not found	71	Not found	120	Circalittoral, bathyal
7.	*Biloculinella inflata*	Not found	Not found	82	80	Circalittoral, bathyal
8.	*Biloculinella labiata**	104	Not found	Not found	80	Circalittoral, bathyal
9.	*Brizalina alata**	Not found	200	Not found	65	Circalittoral, bathyal
10.	*Brizalina striatula*	Not found	184	34	30	Infralittoral
11.	*Bulimina aculeata**	Not found	200	Not found	55	Circalittoral, bathyal
12.	*Bulimina elongata*	Not found	115	25	16	Infralittoral, circalittoral
13.	*Cassidulina carinata**	50	200	Not found	70	Circalittoral, bathyal
14.	*Connemarella rudis**	Not found	54	Not found	22	Circalittoral
15.	*Favulina hexagona**	Not found	115	Not found	22	60
16.	*Globocassidulina subglobosa**	143	200	Not found	80	Circalittoral, bathyal
17.	*Lagena laevis*	Not found	Not found	Not found	30	60
18.	*Lagena nebulosa**	Not found	Not found	Not found	73	Circalittoral, bathyal
19.	*Lagenammina fusiformis*	Not found	82	62	Not found	Not found
20.	*Lenticulina gibba**	Not found	Not found	Not found	40	55
21.	*Nonionella turgida*	Not found	88	Not found	25	40
22.	*Planulina ariminensis**	143	Not found	Not found	77	Circalittoral, bathyal
23.	*Pyrgo elongata*	Not found	Not found	Not found	50	70
24.	*Pyrgo inornata**	Not found	Not found	Not found	50	Circalittoral, bathyal
25.	*Rectuvigerina phlegeri*	Not found	115	57	20	48
26.	*Siphotextularia concava**	Not found	71	Not found	50	Circalittoral, bathyal
27.	*Valvulineria bradyana*	Not found	184	75	50	Circalittoral, bathyal

Source: From previously unpublished data of the authors.
Notes: *Present in cores but absent in live assemblages.
**Circalittoral 40–200 m, bathyal 200–1000 m (Sgarella and Moncharmont, 1993).

to a sample can change a true age of 20,000 yr to an apparent age of 16,500 yr.

To minimize these uncertainties, all material that could be considered as reworked (e.g., foraminifera and detritus of mollusk shells) was removed before the analysis as recommended by Taylor (1987). A benefit of this careful work is reflected in the proper and consistent positioning of ages in a stratigraphic sequence (e.g., Ki-10411 and PTA 6935) and in the steady increase of ages down the core with the exception of the top sample in core 51 (0–2 cm) (Table 1).

Water Mass Stratification

The ^{18}O values of the surface water for the late Pleistocene to middle Holocene in Iskenderun Bay are more negative (lighter) compared to those from the Levantine basin today (–1.42 to –0.6‰; Sperling et al., 2003). They are totally different from those of recent surface water in the Mediterranean Sea (1.5‰ to 2‰), the Marmara Sea (0.1‰ to 1.9‰), and the Black Sea (–3.0‰ to –3.5‰; Schmidt et al., 1999; Aksu et al., 2002). However, they are close to the Caspian Sea values (–1.5‰ to

–2‰; Schmidt et al., 1999), which are characterized by low salinity (average 14‰; Yanko, 1990).

The oxygen isotopic data in foraminiferal tests indicate strong water mass stratification between the horizons dated at 5000 and 13,000 bp. The relatively low oxygen values of planktonic foraminifera (–2.03‰ to –0.17‰; Spezzafferri et al., 2003) reflect warmer and relatively low-salinity surface water. In contrast, the significantly higher ^{18}O values of benthic foraminifera (0.2‰ to 1.1‰; Spezzafferri et al., 2003) reflect colder and more saline bottom water. Similar observations were previously documented by Spezzafferri et al. (2000) for core 29 (3790–5280 yr BP), in which the ^{18}O of the planktonic foraminifera (*G. ruber*) was negative (–1.75‰ to –1.12), whereas that of the benthic foraminifera (*B. marginata* and *B. aculeata*) was positive (0.94‰ to 1.35‰).

Similar conclusions are derived from the ^{13}C values. Those of the planktonic foraminifera (0.88‰ to 1.75‰; Spezzafferri et al., 2000) are higher than those of the benthic foraminifera (–0.61 to –0.06; Spezzafferri et al., 2000), suggesting that the surface water was nutrient-depleted compared with deeper water, and hence were marked by the relatively higher carbon isotopic values. It appears that the late Pleistocene to Holocene planktonic and benthic foraminifera recorded in the cores tapped two different reservoirs of dissolved inorganic carbon associated with the two-layered vertical water mass structure.

The amount of C_{org} in the cores ranges between 0.2% and 2.4% (average 1.1%; Table 1; Figs. 4A–8A), in general higher than that of the surface sediments (0.3%–0.8%, average 0.6%) reported by Ergin et al. (1996), and reflects some oxygen depletion of the bottom due to water stratification, as indicated by the isotopic evidence in foraminifera. The highest value of C_{org}, 2.4%, was calculated in core 138 (7570 yr bp), located at the bay entrance, and corresponds to the time of sapropel S1 deposition in the eastern Mediterranean (Vergnaud-Grazzini et al., 1977). However, there are no sapropels in these cores, because no sapropel formation was possible shallower than 400 m (Shaw and Evans, 1984). In addition, benthic foraminifera are abundant and diverse (174 calcareous and 8 agglutinated species), indicating normal marine sedimentation through all cores. Elucidation of the reasons for late Pleistocene–Holocene water mass stratification is beyond the scope of this work and requires additional study.

Depositional Environment

When plotted on the bathymetrical map, the lithotypes and associated foraminiferal assemblages indicate that they are the result of various depositional microenvironments that do not have consistent distribution on the bay floor. For example, northwest currents distribute sediments along the coast (Ergin et al., 1996), a process clearly reflected by the truncated pattern of deltaic fine-grained sediments and their passage to the coarse belt somewhere around the latitude of the town of Yumurtalik (Fig. 2). Although the coarseness of the sediments increases with the distance from the Ceyhan River, their distribution is patchy. A possible reason for this is an inconsistency in the bottom morphology due to the presence of the stair-case terraces (e.g., T1) and intermediate depressions (e.g., T1-T2). The terraces, in fact, are "reeflike" structures covered by "coralligenous" substrate, sometimes with a foraminiferal assemblage dominated by larger foraminifer *A. lobifera* (Basso and Spezzaferri, 2000). Interestingly, despite the close geographical proximity of T1, T2, and T3, they are inhabited by different foraminiferal assemblages. The T1 assemblage is dominated by *A. lobifera,* indicating favorable conditions for reef growth. A dramatic decrease in abundance of *A. lobifera* on T2 and its full disappearance on T3 most probably shows marginal environmental conditions for reef growth (Hallock, 1996, 2000), likely due to a rapid decease in depth and development of the seaweed *Sargassum vulgare* C. Agardhr as indicated by the dominance of *P. spinigera* (Bresler and Yanko, 1995a,b). There are no *A. lobifera* present in the cores where there are no sediments younger than ~5000 yr bp. Therefore, we can assume that "reeflike" structures in Iskenderun Bay are rather young phenomena that developed quite recently in some areas of the floor.

The T2-T3 assemblage is totally different and consists of a mixture of species (Fig. 3) with contrast microhabitats: *A. pulchella* usually inhabits detritic substrate (Sgarella and Moncharmont Zei, 1993), whereas *T. bocki* prefers silty bottoms (Basso and Spezzaferri, 2000). This may indicate instability of the depositional environment.

Inconsistency in the depositional environment is seen not only in the coastal zone but in the center of the bay as well. A big "island" of coarse sediments (BM, Fig. 2) contains a bottom foraminiferal assemblage that includes a mixture of coarse sand dwellers, *C. bradyi, A. pulchella,* and *T. marioni* and silt-clay inhabitants, e.g., *G. lactea* (AVICENNE Annual Report, 1995; Basso and Spezzaferri, 2000). This assemblage is totally different from others in the surrounding area.

Thus, the present floor of the bay is characterized by variable depositional environments expressed bathymetrically, lithologically, and microfaunistically, with no sediments younger that ca. 5000 yr bp.

Lithologically, the cores are rather similar, dominated by fine-grained sediments with rather uniform C_{org} and $CaCO_3$. An exception is core 16, which has a much higher content of coarse fraction and $CaCO_3$. Despite the apparent sedimentological uniformity in the cores, the foraminiferal assemblages exhibit a definite pattern of decreasing P/B, decreasing percentage of RDS, and increasing percentage of *A. tepida,* which is widely used as an indicator of Quaternary shallow facies of various intercontinental basins (e.g., Cita and Zocchi, 1978; Yanko, 1990), upward in all cores. These parameters indicate a shallowing of the bay from the late Pleistocene to the Holocene.

Sedimentation History

Based on geophysical evidence, Aksu et al. (1992) assumed a constant sediment yield through the Quaternary, suggesting

that the basin had been continuously subsiding at a rate of 0.33×10^{-3} m yr^{-1}. If this is correct, we would expect ~3.3 m of subsidence during the Holocene (0.33×10^{-3} m yr$^{-1} \times 10{,}000$ yr = 3.3 m). Instead, direct chronological control of core material yields a much lower sedimentation rate (all lower than 1.2 m per 10, 000 yr). In addition, the process of sediment yield was not constant, as can be seen by fluctuations in the sedimentation rate, such as the negative rate seen since ~5000 yr bp (Table 1).

Why is the rate of sedimentation so low? It is well known that modern shelf environments receive a rather wide variety of sediment types, both from terrigenous influx and from within the basin of accumulation. If we consider the possible variations in sediments, the foremost factor would be "the abundance of significant rivers to provide a means of (sediment) transportation to the sea" (Davis, 1972). The Ceyhan River is the only main source of river-borne sediments into the bay. This river did not always discharge its river-borne material directly into the bay, but rather discharged it into the Mediterranean Sea (Skelton, 1969; Spezzaferri et al., 2000). In addition, long-shore currents could have removed part of the sediments from the bay (Ergin et al., 1996). Thus, a possible lack of terrigenous material could explain why the sedimentation rate is so low. However, it cannot explain why there are no sediments younger that 5000 yr bp in the core-top samples, particularly in the center of the bay, where the influence of long-shore currents is nonexistent.

Thus, there are strong variations in lithotypes, foraminiferal assemblages, and appearance of older sediments on the bay floor, suggesting that sedimentation in the bay was discontinuous with regard to mode and conditions of deposition. Further evidence of discontinuous sedimentation is indicated by differences in isotopic values.

Tectonic Activity and Uplift

Planktonic foraminifera are distributed throughout the cores, although they are absent in the bay today despite that the fact the bay has standard salinity for the eastern Mediterranean and freely exchanges water with the open sea. Apparently, the shallow (maximum 87 m) depth of the bay is a barrier factor. Thus, the bay must have been deeper in the late Pleistocene–early Holocene than it is now. At 13,500 yr bp (core 138, 60–62 cm, Fig. 8A), the global sea level was about 100 m below the present level (Fairbanks, 1989). With this drop in sea level, the deepest sediment in core 138 should be located on land. Instead, it exhibits normal marine foraminiferal assemblages with a high number of benthic species, diversity (Table 1), and abundant $CaCO_3$ throughout. At that time, the depth of the bay should have been at least 100 m. It must have been uplifted with an average speed of 0.5–1.5 cm yr^{-1} from the late Pleistocene to the present (Koral et al., 2001).

Irregularities in bottom morphology, lithology, and foraminiferal distribution coincide with the location of en echelon faults (Fig. 2) detected by previous seismic (e.g., Aksu et al., 1992), GPS, neotectonic, and seismicity data (Barka et al., 1999) and by sonar readings (e.g., Buyukasikoglu, 1979; Osmansahin et al., 1986) indicating tectonic influence on the depositional environment.

As the bay was faulted into slices, local microenvironments of different depth and isolated subbasins were created. Similar phenomena were documented recently in Izmit Bay (in the Sea of Marmara) during the 1999 earthquake, which displaced fault blocks and produced local subsidence and uplift along the coastline and in the bay (Öztürk et al., 2000; Koral, 2006).

Thus, tectonic activity and active faulting on the floor of Iskenderun Bay can explain irregularities in the foraminiferal distributions. The depositional environments on the different blocks, as recorded in the cores, could create the potential for developing different assemblages due to the lack of seafloor continuity between sites, despite being taken from similar depths. Likewise, the different rates and modes of faulting might create discontinuous ecological conditions, leading even to degradation of reeflike terraces. This activity can also explain why live and fossil foraminiferal assemblages from the core-top samples are totally different (Figs. 4B and C through 8B and C), because there should not be obvious differences in the parameters between live and dead populations (Scott and Medioli, 1980).

Tectonic activity and active faulting can also explain the irregular bottom morphology of the bay. For instance, while the "bump" on the northwest side of the bay was probably formed by deltaic sediments (Fig. 1B), the "bump" on the southeast side (Fig. 1F) seems to have a tectonic origin. A similar "bump" is present on the seismic profile obtained by Ergin et al. (1998, their Fig. 4) in Iskenderun Bay. It is considered a relict bottom feature (a paleoshore?) that was formed under the last stands of sea level conditions (Ergin et al., 1998) and tectonically uplifted later (Ergin et al., 1997), similar to that on the southern coast of the Gulf of Corinth, Greece (Pirazzoli et al., 2004). Of course, the role of deep currents in the formation of the "bumps" cannot be ruled out. However, no information is available so far.

Tectonic activity and active faulting can explain the disturbance seen in the sedimentary column, such as the age inversion that is encountered at the top of core 51. The older deposits must have slumped down from a nearby block of higher elevation when the younger sediments were being deposited. Examples of such slumps were also observed during the 1999 earthquake in Izmit Bay (Öztürk et al., 2000).

Tectonic uplift can explain irregularities in the sedimentation process, such as the occurrence of coarse sediments in the center of the bay, a large variety of lithotypes on the bay floor, and the low rate and periodic cessation of sedimentation seen in the cores. The amount of terrigenous material is directly proportional to the tectonic activity (Frolov, 1993). Erosional unconformities in the sediment column reflect the location of regional and local uplifts, which sometimes decrease sediment thickness to zero (Hain and Lomidze, 1995).

The tectonic uplift is in agreement with the geophysical data. Most of the basin floor is characterized by a broad nega-

tive Bouguer gravity anomaly that is in contrast to the positive anomalies that characterize the adjacent easternmost Mediterranean Sea floor (Woodside, 1977; Makris and Wang, 1994; Koral et al., 2001). This suggests that this fairly large sedimentary basin is undercompensated and potentially buoyant. A long-lasting (<780 k.y.) tectonic uplift in the head of Iskenderun Bay is supported by paleomagnetic study of young volcanics (Gürsoy et al., 2003).

Iskenderun Bay occurs in a geological setting where faulting and uplift are expected to be significant tectonic processes. There are numerous faults striking subparallel and subdiagonal to the main axis of the bay itself (Perinçek and Çemen, 1990; Aksu et al., 1992, 1999; Ergin et al., 1998), and there are remnants of raised beaches along the bay margins (Şengör et al., 1985; Westaway and Arger, 1996). The bay occurs in the region where convergence between the Arabian and Anatolian plates led to the collision, crustal thickening, and uplift of Eastern Anatolia by up to 2 km (Şengör et al., 1985; Westaway and Arger, 1996). Likewise, the uplift of Cyprus was formed by the collision and underthrusting of the Eratosthenes seamount with continental Anatolia (e.g., Robertson, 1998).

Thus, tectonic uplift related to fault movements is the most plausible explanation, especially taking into consideration the converging tectonic setting of the Turkish and African plates and the fact that uplift is expected in a convergence zone (Kronfeld et al., 1996; Koral et al., 1999, 2001). Indeed, similar coseismic tectonic activity and associated subsidence and uplift of the sea floor were documented recently in the similar setting of Izmit Bay during the 1999 earthquake (Öztürk et al., 2000; Koral, 2006).

CONCLUSIONS

Iskenderun Bay has an irregular bottom morphology and displays complex and irregular depositional and foraminiferal relationships. These irregularities include (1) the stair-case morphology of the bay floor, (2) a large variety of lithotypes and foraminiferal assemblages, (3) a hiatus between live and fossil foraminiferal assemblages, (4) differences in foraminiferal assemblages in the cores collected from comparable depths and sedimentological conditions, and (5) the absence of young sediments in the core-top samples. Taken together, they indicate the occurrence of local subbasins whose floors lay at different elevations and moved at different rates compared to their neighbors. Hence, these abnormalities could be explained largely by tectonic activity and uplift. The tectonics has created an apparently very complex environmental situation represented by distinct foraminiferal assemblages and lithotypes. It is further suggested that Iskenderun Bay may constitute a model for other tectonically active regions where the foraminiferal data may exhibit similarly complex patterns. Lack of correlation between cores taken at similar depths, as well as in downcore profiles, may be the result of the effects of differential basinal movement, slumping, and overturning. In such cases, not only is a very precise knowledge of the foraminiferal ecology of prime importance for unraveling the paleoenvironment, but it is also indispensable to establish a detailed lithology and radiocarbon-based chronology.

ACKNOWLEDGMENTS

This study was supported by an EU grant (AVICENNE Program, AVI CT92-0007). Our special thanks to the officers and crew of the R/V *Koca Piri Reis* for their assistance and data acquisition. D. Basso, E. Meriç, and S. Spezzafferri are gratefully acknowledged for their collaboration during cruises AVI-2 and AVI-4. M. Ergin, University of Ankara, Turkey, and C. Ioakeim, Institute of Geology and Mineral Exploration, Greece, are gratefully acknowledged for their scientific review of the manuscript. We sincerely thank J.C. Vogel, Quaternary Dating Research Unit, South Africa, and N. Kovalyukh and V. Skripkin, Kiev Radiocarbon Laboratory, Ukraine, for radiocarbon analysis and constructive discussion of obtained results. We thank J. Kronfeld, Tel Aviv University, Israel, for his comments and criticism.

REFERENCES CITED

Aksu, A.E., Ulug, A., Piper, D.Y.P., Konuk, Y.T., and Turgut, S., 1992, Quaternary sedimentary history of Adana, Cilicia and Iskenderun basins: Northeast Mediterranean Sea: Marine Geology, v. 104, p. 55–71, doi: 10.1016/0025-3227(92)90084-U.

Aksu, A.E., Hiscot, R.N., and Yaşar, D., 1999, Oscillating Quaternary water levels of the Marmara Sea and vigorous outflow into the Aegean Sea from the Marmara Sea–Black Sea drainage corridor: Marine Geology, v. 153, p. 275–302.

Aksu, A.E., Hiscott, R.N., Kaminski, M.A., Mudie, P.J., Gillespie, T., Abrajano, T., and Yaşar, D., 2002, Last Glacial-Holocene palaeoceanography of the Black Sea and Marmara Sea: Stable isotopic, foraminiferal and cocolith evidence: Marine Geology, v. 190, p. 119–149, doi: 10.1016/S0025-3227(02)00345-6.

Andrews, J.T., and Miller, G.H., 1980, Dating Quaternary deposits more than 10,000 years old, *in* Cullingford, R.A., et al., eds., Timescales in Geomorphology: New York, John Wiley & Sons, p. 263–287.

AVICENNE Annual Report, 1993, Benthic foraminifera as indicators of heavy metal pollution: A new kind of biological monitoring for the Mediterranean Sea: Contract no. AVI CT92–0007, Tel Aviv University, Israel, 41 p.

AVICENNE Annual Report, 1995, Benthic foraminifera as indicators of heavy metal pollution: A new kind of biological monitoring for the Mediterranean Sea: Contract no. AVI CT92–0007, Tel Aviv University, Israel, 270 p.

AVICENNE Annual Report, 1996, Benthic foraminifera as indicators of heavy metal pollution: A new kind of biological monitoring for the Mediterranean Sea: Contract no. AVI CT92–0007, Tel Aviv University, Israel, 167 p.

Bal, Y., and Demirkol, C., 1987, Coastline changes in eastern Mediterranean, Turkey: Earth Science Review, Engineering Faculty, Istanbul University, v. 6, p. 69–91.

Barka, A.S., Akyüz, S., and Altunel, E., 1999, Adana çevresinin Güncel Tectoniği ve 1998 Adana Depremi, *in* Proceedings, Aktif Tectonic Araştrma Grubu Toplantisi: Istanbul Technical University, Istanbul, Turkey, p. 20–31 (in Turkish).

Basso, D., and Spezzaferri, S., 2000, The distribution of living (stained) benthic foraminifera in Iskenderun Bay (eastern Turkey): A statistical approach: Bollettino Società Paleontologica Italiana, v. 39, p. 359–379.

Basso, D., Spezzaferri, S., Yanko, V., Koral, H., and Avsar, N., 1994, Cruise AVI-

II 93: Preliminary data from Iskenderun Bay (Turkey): Rendiconti Accademia Lincei, v. 9, p. 233–245.

Bernhard Weninger, F., 1986, Acta Interdisciplinaria Archeologica IV: Nitra, Slovenska (SK), p. 11–53.

Bozkurt, E., 2001, Neotectonics of Turkey: A synthesis: Geodynamica Acta, v. 14, p. 3–30, doi: 10.1016/S0985-3111(01)01066-X.

Bresler, V., and Yanko, V., 1995a, Acute toxicity of heavy metals for benthic epiphytic foraminifera *Pararotalia spinigera* (Le Calvez) and influence of seaweed-derived DOC: Environmental Toxicology and Chemistry, v. 14, p. 1687–1695.

Bresler, V., and Yanko, V., 1995b, Chemical ecology: A new approach to study living benthic epiphytic foraminifera: Journal of Foraminiferal Research, v. 25, no. 3, p. 267–279.

Buyukasikoglu, S., 1979, Properties of the Eurasian-African plate boundary in southern Anatolia and the eastern Mediterranean, based on seismological data [Ph.D. thesis]: Istanbul Technical University, Istanbul, 75 p. (in Turkish).

Capitani, L., Basso, D., and Lacerenza, S., 2000, Distribution of heavy metals in the sediments of Iskenderun Bay (Turkey): Geochemistry, v. 60, p. 209–230.

Cimerman, F., and Langer, R., 1991, Mediterranean foraminifera: Ljubljana, Slovenska, 215 p.

Cita, M.B., and Zocchi, M., 1978, Distribution patterns of benthic foraminifera on the floor of the Mediterranean Sea: Oceanologica Acta, v. 1, p. 445–462.

Cullen, H.M., Kaplan, A., Arkin, P.A., and de Menocal, P.B., 2002, Impact of the North Atlantic oscillation on Middle Eastern climate and streamflow: Climatic Change, v. 55, no. 3, p. 315–338, doi: 10.1023/A:1020518305517.

Davis, R.A., Jr., 1972, Principles of oceanography: Reading, Massachusetts, Addison-Wesley, 434 p.

Dewey, J.F., Hempton, M.R., Kidd, W.S.F., Şaroğlu, F., and Şengör, A.M.C., 1986, Shortening of continental lithosphere: The neotectonics of eastern Anatolia, a young collision zone, *in* Coward, M.P., and Ries, A.C., eds., Collision tectonics: Geological Society of London Special Publication 19, p. 3–36.

Ergin, M., Kazan, B., and Ediger, V., 1996, Source and depositional controls on heavy metal distribution in marine sediments of the Gulf of Iskenderun, Eastern Mediterranean: Marine Geology, v. 133, p. 223–239, doi: 10.1016/0025-3227(96)00011-4.

Ergin, M., Kazanci, N., Varol, B., Ileri, Ö., and Karadenizli, L., 1997, Sea-level changes and related depositional environments on the southern Marmara shelf: Marine Geology, v. 140, p. 391–403, doi: 10.1016/S0025-3227(97)00029-7.

Ergin, M., Kazan, B., Yücesoy-Eryılmaz, F., Eryılmaz, M., and Okyar, M., 1998, Hydrographic, deltaic and benthogenic controls of sediment dispersal in the Gulf of İskenderun, SE Turkey (E. Mediterranean): Estuarine, Coastal and Shelf Science, v. 46, p. 493–502, doi: 10.1006/ecss.1996.0231.

Fairbanks, R.G., 1989, A 17, 000-year glacio-eustatic sea-level record: Influence of glacial melting rates on the Younger Dryas event and deep-ocean circulation: Nature, v. 342, p. 637–642, doi: 10.1038/342637a0.

Folk, I.R., 1974, Petrology of sedimentary rocks: Tulsa, Oklahoma, Hemphil, 182 p.

Frolov, V.T., 1993, Litologia (Lithology): Moscow State University, v. 2, 430 p. (in Russian).

Frolov, V.T., 1995, Litologia (Lithology): Moscow State University, v. 3, 352 p. (in Russian).

Grillot, H., Béouinot, J., Boucetta, M., and Rouquetta et Arnost Sima, C., 1964, Méthodes d'analyse quantitative appliquées aux roches et aux prélèvements de la prospection géochimique: Mémoires du BRGM 30, 225 p.

Gürsoy, H., Tatar, O., Piper, J.D.A., Heimann, A., and Mesci, L., 2003, Neotectonic deformation linking the east Anatolian and Karataş-Osmaniye intracontinental transform fault zones in the Gulf of Iskenderun, southern Turkey, deduced from paleomagnetic study of the Ceyhan-Osmaniye volcanics: Tectonics, v. 22, no. 6, 1067, p. 6–1 to 6–12.

Hain, B.E., and Lomidze, M.G., 1995, Geotectonica s osnovami geodinamiki (Geotectonics with basics of geodynamics): Moscow State University, Moscow, 480 p. (in Russian).

Hall, J., Udintsev, G.B., and Odinokov, Ju.Ju., 1994, The bottom relief of the Levantine Sea, *in* Krasheninnikov, V.A., and Hall, J., eds., Geological structure of the North-Eastern Mediterranean (Cruise 5 of the Research Vessel "Akademik Nikolai Strakhov"): Jerusalem, Historical Productions–Hall Ltd., p. 5–32.

Hallock, P., 1996, *Amphistegina* (Foraminiferida) densities as a practical, reliable, low-cost indicator of coral reef vitality, *in* Crosby, M.P., et al., eds., A Coral Reef Symposium on Practical, Reliable, Low Cost Monitoring Methods for Assessing the Biota and Habitat Conditions of Coral Reefs, January 26–27, 1995: Silver Spring, Maryland, Office of Ocean and Coastal Resource Management, National Oceanic and Atmospheric Administration, p. 37–43.

Hallock, P., 2000, Larger foraminifera as indicators of coral-reef vitality, *in* Martin, R., ed., Environmental micropaleontology: New York, Kluwer, p. 121–150.

Hottinger, L., Halicz, E., and Reiss, Z., 1993, Recent foraminiferida from the Gulf of Aquaba, Red Sea: Liubliana, Slovenska Akademia Znanosti in Umelosti, 179 p.

Iyiduvar, Ő., 1986, Hydrographic characteristics of Iskenderun Bay [Ph.D. thesis]: Institute of Marine Sciences, METU, Erdemli, Içel, 157 p.

Jorissen, F.J., 1987, The distribution of benthic foraminifera in the Adriatic Sea: Marine Micropaleontology, v. 12, p. 21–48, doi: 10.1016/0377-8398(87)90012-0.

Kempler, D., 1994, An outline of Northeastern Mediterranean tectonics in view of Cruise 5 of the Akademik Nikolai Strakhov, *in* Krasheninnikov, V.A., and Hall, J., eds., Geological structure of the North-Eastern Mediterranean (Cruise 5 of the Research Vessel "Akademik Nikolai Strakhov"): Jerusalem, Historical Productions–Hall Ltd., p. 277–293.

Koral, H., Kronfeld, J., Avsar, N., Yanko, V., and Vogel, J.C., 1999, Major recent tectonic uplift in Iskenderun Bay, northeastern Mediterranean Sea: European Union of Geosciences Annual Meeting, Strasburg, Abstracts, p. 406.

Koral, H., Kronfeld, J., Avsar, N., Yanko, V., and Vogel, J.C., 2001, Major recent tectonic uplift in Iskenderun Bay, Turkey: Radiocarbon, v. 43, p. 957–963.

Koral, H., 2006, Sea-level changes modified the Quaternary coastal lines in the Marmara region, NW Turkey: What about tectonic movements?, *in* Yanko-Hombach, V., Gilbert, A., Panin, N., and Dolukhanov, P., eds., The Black Sea flood question: Changes in coastline, climate, and human settlement: Dordrecht, the Netherlands, Springer-Verlag, p. 571–601.

Kronfeld, J., Yanko, V., Vogel, J.C., Avsar, N., and Koral, H., 1996, Major tectonic uplift in Iskenderun Bay, easternmost Mediterranean Sea: Denver, Geological Society of America Abstracts with Programs, v. 28, p. 395.

Loeblich, A.R., and Tappan, H., 1988, Foraminiferal genera and their classification: New York, Van Nostrand Reinhold Company, 970 p., 847 plates.

Makris, J., and Wang, J., 1994, Bouguer gravity anomalies of the eastern Mediterranean Sea, *in* Krasheninnikov, V.A., and Hall, J., eds., Geological structure of the North-Eastern Mediterranean (Cruise 5 of the Research Vessel "Akademik Nikolai Strakhov"): Jerusalem, Historical Productions–Hall Ltd., p. 87–98.

McKenzie, D.P., 1972, Active tectonics of the Mediterranean region: Geophysical Journal of the Royal Astronomic Society, v. 30, p. 109–185.

Motnenko, I., 1999, Litologia sovremennikh osadkov shelfa Israilia i ikh antropogennoe zagriaznenie (Lithology of recent sediments of Israeli shelf and their anthropogenic pollution) [Ph.D. thesis]: Moscow University, Moscow, 240 p. (in Russian).

Nur, A., and Ben-Avraham, Z., 1978, The eastern Mediterranean and the Levant: Tectonics of continental collision: Tectonophysics, v. 46, p. 297–311, doi: 10.1016/0040-1951(78)90209-3.

Osmansahin, Y., Eksi, F., and Alptekin, Ö., 1986, Seismicity of the Eastern Anatolia and Caucasian regions and its active tectonics: Deprem Araştıma Bült., v. 52, p. 5–41.

Öztürk, H., Koral, H., and Geist, E.L., 2000, Intra-basinal water movements induced by faulting: the August 17, 1999, Gölcük (Izmit Bay) earthquake (Mw = 7.4): Marine Geology, v. 170, p. 263–270, doi: 10.1016/S0025-3227(00)00090-6.

Parker, F.L., 1947–1948, 1958, Eastern Mediterranean foraminifera: Reports of the Swedish Deep-Sea Expedition, v. 8, p. 218–285.

Pelc, V., 1995. Approche méthodologique de la chronométrie ^{14}C de l'Holocène marin en Méditerranée, à partir des tests calcaires (M.Sc. thesis): Université Claude Bernard, Lyon, 47 p.

Perinçek, D., and Çemen, I., 1990, The structural relationship between the East Anatolian and Dead Sea fault zones in southern Turkey: Tectonophysics, v. 172, p. 331–340, doi: 10.1016/0040-1951(90)90039-B.

Pirazzoli, P.A., Stirosb, S.C., Fontugnec, M., and Arnold, M., 2004, Holocene and Quaternary uplift in the central part of the southern coast of the Corinth Gulf (Greece): Marine Geology, v. 212, p. 35–44, doi: 10.1016/j.margeo.2004.09.006.

Polach, H., Golson, J., and Head, J., 1981, Radiocarbon dating: A guide for archaeologists on the collection and submission of samples and age-reporting practices, *in* Connah, G., ed., Australian field archaeology: A guide to techniques: Canberra, Australian Institute of Aboriginal Studies, p. 145–152.

Puseman, K., Nepstad-Thornberry, C., and Klinge, R.E., 2001, Dating bulk soil vs. identified organics at archaeological sites: 66th Annual Meeting of the Society for American Archaeology, New Orleans, Abstracts, p. 304.

Reimer, P.J., and McCormac, F.G., 2002, Marine radiocarbon reservoir corrections for the Mediterranean and Aegean Seas: Radiocarbon, v. 44, p. 159–166.

Robertson, A.H.F., 1998, Tectonic significance of the Eratosthenes Seamount: A continental fragment in the process of collision with a subduction zone in the eastern Mediterranean (Ocean Drilling Program Leg 160): Tectonophysics, v. 298, p. 63–82, doi: 10.1016/S0040-1951(98)00178-4.

Rosholt, J.N., Colman, S.M., Stuiver, M., Damon, P.E., Naeser, C.W., Naeser, N.D., Szabo, B.J., Muhs, D.J., Liddicoat, J.C., Forman, S.L., Machette, M.N., and Pierce, K.L., 1991, Dating methods applicable to the Quaternary, *in* Morrison, R.B., ed., The geology of North America, v. K-2: Boulder, Colorado, Geological Society of America, p. 45–74.

Schlichting, E., and Blume, H.-P., 1966, Bodenkundliches Praktikum: Hamburg und Berlin, Verlag Paul Parey, 209 p.

Schmidt, G.A., Bigg, G.R., and Rohling, E.J., 1999, Global Seawater Oxygen-18 Database: http://www.giss.nasa.gov/data/o18data/.

Scott, D.B., and Medioli, F.S., 1980, Living vs total foraminiferal populations: Their relative usefulness in paleoecology: Journal of Paleontology, v. 54, p. 814–831.

Şengör, A.M.C., and Yılmaz, Y., 1981, Tethyan evolution of Turkey: A plate tectonic approach: Tectonophysics, v. 75, p. 181–241, doi: 10.1016/0040-1951(81)90275-4.

Şengör, A.M.C., Görur, N., and Şaroğlu, F., 1985, Strike-slip faulting and related basin formation in zones of tectonic escape: Turkey as a case study: Society of Economic Paleontology and Mineralalogy Special Publication 27, p. 227–264.

Sgarella, F., and Moncharmont Zei, M., 1993, Benthic foraminifera of the Gulf of Naples (Italy): Systematics and autoecology: Bollettino della Società Paleontologica Italiana, v. 32, p. 145–264.

Shaw, N.F., and Evans, G., 1984, The nature, distribution, and origin of a sapropelic layer in sediments of the Cilica Basin, Northern Mediterranean: Marine Geology, v. 61, p. 1–12, doi: 10.1016/0025-3227(84)90104-X.

Skelton, R.A., 1969, Claudius Ptolomaeus: Geographia, Venice 1511. Amsterdam, Theatrvm Orbis Terrarvm.

Skripkin, V., and Kovalyukh, N., 1998, Recent developments in the procedure used at the SSCER Laboratory for the routine preparation of lithium carbide: Radiocarbon, v. 40, p. 211–214.

Skripkin, V., Kovalyukh, N., Pazdur, A., and Pazdur, M.F., 1994, Highly efficient chemical technology of sample preparation for liquid scintillation, radiocarbon measurements: Annual Reports, 44–100 GLIWICE, Krzywoustego 2 (Poland), p. 49–50.

Sperling, M., Schmiedl, G., Hemleben, Ch., Emeis, K.C., Erlenkeuser, H., and Grootes, P.M., 2003, Black Sea impact on the formation of eastern Mediterranean sapropel S1?: Evidence from the Marmara Sea: Palaeogeography, Palaeoclimatology, Palaeoecology, v. 2957, p. 1–13.

Spezzaferri, S., Basso, D., and Koral, H., 2000, Holocene paleoceanographic evolution of the Iskenderun Bay, South-Eastern Turkey, as a response to river mouth diversions and human impact: Mediterranean Marine Science, v. 1, p. 19–43.

Spezzaferri, S., Yanko-Hombach, V., and Bruchez, S., 2003, Late glacial freshening of the Levantine Basin: Isotopic evidence from Iskenderun Bay: Geological Society of America Abstracts with Programs, v. 35, no. 6, p. 189–216.

Stigter, H.C., de Jorissen, F.J., and Van Der Zwaan, G.J., 1998, Bathymetric distribution and microhabitat partitioning of live (Rose Bengal stained) foraminifera along a shelf to bathyal transect in the southern Adriatic Sea: Journal of Foraminiferal Research, v. 28, p. 40–65.

Taylor, R.E., 1987, Radiocarbon dating: A handbook for archaeologists: New York, Academic Press, 212 p.

Tolun, N., and Pamir, H.N., 1975, Explanatory text of the geological map of Turkey: Hatay sheet: Mineral Research and Exploration Institute (MTA) of Turkey, Ankara, 99 p., scale 1:500,000 (in Turkish).

Van Der Plicht, J., 1993, The Groningen radiocarbon calibration program: Radiocarbon, v. 35, p. 231–237.

Vergnaud-Grazzini, C., Ryan, W.B.F., and Cita, M.B., 1977, Stable isotopic fractionation, climate change and episodic stagnation in the eastern Mediterranean during the Late Quaternary: Marine Micropaleontology, v. 2, p. 353–370, doi: 10.1016/0377-8398(77)90017-2.

Vogel, J.C., and Marais, M., 1971, Pretoria radiocarbon dates, I: Radiocarbon, v. 13, p. 378–394.

Westaway, R., and Arger, J., 1996, The Golbasi basin, southeastern Turkey: A complex discontinuity in a major strike-slip fault zone: Journal of the Geological Society of London, v. 153, p. 729–743.

Woodside, J.M., 1977, Tectonic elements and the crust of the eastern Mediterranean Sea: Marine Geophysical Research, v. 3, p. 317–354, doi: 10.1007/BF00285658.

Yanko, V., 1989, Chetvertichnie foraminiferi Ponto-Caspia (Chernoe, Azovskoe, Caspiiskoe i Aral'skoe moria): Taxonomia, biostratigrafia, istoria razvitia, ecologia (Quaternary foraminifera of the Pontic-Caspian region [the Black Sea, Sea of Azov, Caspian Sea and Aral Sea]: Taxonomy, biostratigraphy, history, ecology) [D.Sc. thesis]: Moscow State University, Moscow, 2 volumes, 734 p., 70 plates (in Russian).

Yanko, V., 1990, Stratigraphy and palaeogeography of marine Pleistocene and Holocene deposits of the Southern Seas of the USSR: Memorie della Società Geologica Italiana, v. 44, p. 167–187.

Yanko, V., and Troitskaya, T., 1987, Pozdnechetvertichnie foramiferi Chernogo moria (Late Quaternary foraminifera of the Black Sea): Moscow, Nauka, 111 p. (in Russian, with English abstract).

Yanko, V., Ahmad, M., and Kaminski, M., 1998, Morphological deformities of benthic foraminiferal tests in response to pollution by heavy metals: Implications for pollution monitoring: Journal of Foraminiferal Research, v. 28, no. 3, p. 177–200.

Yılmaz, Y., and Gürer, F., 1996, The geology and evolution of the Missis-Andrin Belt, around Andirin (Kahraman-maras): Turkish Journal of Earth Sciences, v. 5, p. 39–56.

Yılmaz, A., Bastürk, Ö., Saydam, C., Ediger, D., Yılmaz, K., and Hatipoglu, E., 1992, Eutrophication in Iskenderun Bay, northeastern Mediterranean: The Science of the Total Environment, supplement, p. 705–717.

Manuscript Accepted by the Society 30 December 2005